Research Article

Exact Free Vibration Analysis for Plate Built-Up Structures under Comprehensive Combinations of Boundary Conditions

Xiang Liu,[1,2,3,4] **Chen Xie,**[1,2,3] **and Han-cheng Dan** [ID] [5]

[1]*Key Laboratory of Traffic Safety on Track (Central South University), Ministry of Education, Central South University, Hunan, Changsha 410075, China*
[2]*Joint International Research Laboratory of Key Technology for Rail Traffic Safety, Hunan, Changsha 410075, China*
[3]*School of Traffic & Transportation Engineering, Central South University, Hunan, Changsha 410075, China*
[4]*State Key Laboratory of High Performance Complex Manufacturing, Central South University, Hunan, Changsha 410075, China*
[5]*School of Civil Engineering, Central South University, Hunan, Changsha 410075, China*

Correspondence should be addressed to Han-cheng Dan; danhancheng@csu.edu.cn

In this research, an exact dynamic stiffness model for spatial plate built-up structures under comprehensive combinations of different boundary conditions is newly proposed. Dynamic stiffness formulations for plate elements with 16 different types of supported opposite edges and arbitrarily supported boundary conditions along other edges are developed, which makes the dynamic stiffness method (DSM) more applicable to engineering problems compared to existing works. The Wittrick–Williams algorithm of the DSM is applied with the explicit expressions of the J_0 count for plate elements under all above support conditions. In return, there is no need to refine the element in the DSM, and thus, it becomes immensely efficient. Moreover, the present theory is applied for exact free vibration analysis within the whole frequency range of three built-up structures which are commonly encountered in engineering. The results show that the DSM gives exact results with as much as 100-fold computational efficiency advantage over the commercial finite element method. Besides, benchmark results are also provided.

1. Introduction

Plate built-up structures normally serve as the main structures in a wide range of areas, such as rail transit, aerospace, automotive, and civil engineering. Excessive vibration and noise not only reduce the comfort of people but also may cause fatigue to structures, whereas free vibration properties are one of the most important and fundamental concerns in structural design. Therefore, it is virtually important to find efficient and accurate methods for the free vibration analysis of plate built-up structures. There are many well-developed analysis methods such as the finite element method (FEM) and boundary element method (BEM) for low-frequency vibration analysis and statistical energy analysis (SEA) for the high-frequency range. However, some built-up structures are usually characterized by a complex vibration form in which both long- and short-wavelength deformations occur simultaneously. As a result,

both the FEM/BEM and SEA become inapplicable to this midfrequency problem, and alternative methods should be resorted to the study [1].

One of the powerful alternatives is the dynamic stiffness method (DSM), whose shape functions are the exact general solutions of the governing differential equations (GDEs). Therefore, the exact natural frequencies and modal shapes of the structures within the whole frequency range can be obtained. Moreover, another benefit of the DSM is that the structure does not need to be meshed unless the geometry and material are discontinuous, which indicates that an infinite number of natural modes can be solved by using extremely few degrees of freedom (DOFs). Thus, it is obvious that the DSM is very efficient compared to the FEM. It is worth mentioning that compared to other analytical methods, the DSM applies an efficient and robust algorithm, the Wittrick–Williams (WW) algorithm [2], which guarantees that no natural frequency is missed. In addition, the

DSM elements can be assembled directly just as the FEM to model the complex structure.

The DSM was originally proposed by Kolousek [3] in 1941. Subsequently, many authors [4–9] have done numerous works on the DSM of beam structures, which greatly promote the application of the DSM in engineering problems. In addition, there are some studies on the dynamic analysis of plate structures using dynamic stiffness theory. For example, Williams and Wittrick [10] performed vibration and buckling analysis on isotropic and anisotropic plates and compiled computer programs called VIPASA [10], VICON [11], and VICONOPT [12, 13]. The method is later applied by Williams and Banerjee [14] to compute the modal densities of structures. Bercin et al. [15, 16] developed the dynamic stiffness matrices of plate built-up structures and studied the contribution of inplane modes in the mid-high-frequency domain. Boscolo and Banerjee [17] developed the explicit expressions of the dynamic stiffness matrices for out-of-plane free vibration using classical plate theory and first-order shear deformation theory, respectively. Wu et al. [18–20] applied the dynamic stiffness method for power flow analysis of plate built-up structures. However, all above researches are restricted to plates with two opposite sides simply supported in one form, where the opposite edges should be the so-called "SS1" type for inplane vibration (normal stress and tangential displacement are zero) and "S" for out-of-plane vibration (transverse displacement and moment are zero). However, in engineering applications, there are more types of boundary conditions which cannot be modeled by the above boundary conditions. The Ritz method was used to study the free vibration of completely free rectangular shallow shell structures [21]. It is a weak-form-based method because the GDEs and boundary conditions are sometimes satisfied in a variational sense [22]. In contrast, the superposition method adopted by Gorman et al. [23–27] can obtain the solutions that satisfy both GDEs and boundary conditions in a strong manner. This method was applied to study the exact solution of the plates under various boundary conditions and pointed out two types of simply supported boundary conditions for inplane vibration [28]. Xing et al. [29–32] developed the exact modal solutions for inplane vibration of individual plates with opposite edges SS1 and SS2 (tangential stress and normal displacement are zero) supported and transverse vibration with opposite edges simply supported (S) and/or guided (G). However, all existing researches [29–32] focus on single plates and are inapplicable to plate assemblies. To the best knowledge of the authors, there have not been exact dynamic stiffness formulations for plate assemblies with the opposite edges supported by "G" and "SS2" boundary conditions.

Furthermore, when applying the DSM to modal analysis, there are many methods for obtaining the eigenvalues from the DS matrix, like the determinantal methods [15, 16, 18–20], but they are inefficient and meanwhile very likely to miss some modal solutions [28]. These shortcomings can be overcome by the Wittrick–Williams (WW) algorithm, which is an extremely efficient and accurate algorithm for the DSM; however, the J_0 count in the algorithm is an important and difficult problem [33]. J_0 is the number of natural frequencies below the trial frequency when all the nodes of the structure are clamped. A majority of researches [17, 34–36] discretized the structure into a finer dynamic stiffness mesh to ensure that J_0 is equal to zero, which greatly reduces the computational efficiency, and the merit of the DSM is not brought into full play.

This paper develops the dynamic stiffness formulations for plate elements with opposite edges supported by any combinations of S1, S2 for inplane vibration and S, G for out-of-plane vibration and arbitrarily supported boundary conditions along other edges. That is to say, there are 16 kinds of opposite-edge-supported condition combinations, i.e., four for inplane vibration, S1-S1, S2-S2, S1-S2, and S2-S1, and another four for transverse vibration, S-S, G-G, S-G, and G-S. As a consequence, the number of boundary conditions of a plate element considered by the DSM increases from 100 to 1600, which makes the DSM more applicable to engineering problems. More details about the opposite-edge-supported boundary conditions are given in Section 2.1.

At the same time, the mode count (J_0) of the WW algorithm under all possible opposite-edge-support conditions is formulated analytically in this study. Thus, minimal degrees of freedom are necessary for the DSM to model complex structures, which makes the DSM an efficient analytical method within the whole frequency ranges. This work greatly enhances the superiority of the DSM over the FEM in computational efficiency. The current research can also be used for power flow analysis and puts forward efficient analytical solutions for important parameters (modal density, coupling loss factor [37], etc.) for other methods like the statistical energy analysis (SEA) method.

This paper is organized as follows: In Section 2.1, the boundary conditions in this research are detailed. Then, the formulations of dynamic stiffness matrices for inplane vibration under different types of opposite-edge-support conditions are developed (Section 2.2). Next, the expressions for three different support conditions of out-of-plane vibration are presented (Section 2.3). Section 2.4 shows the assembly procedure of the plate elements. Then, the J_0 formulations are solved in Section 2.5. In Section 3, the natural frequencies of the individual plate for inplane (Section 3.1) and out-of-plane (Section 3.2) vibrations computed by the DSM are presented compared to the FEM solutions. Section 3.3 demonstrates the accuracy and calculational efficiency studies of the DSM on three kinds of plate built-up structures which are widely used in engineering. Finally, some conclusions of this work are drawn in Section 4.

2. Theory

This section describes the development of dynamic stiffness (DS) formulations for a plate element under comprehensive combinations of different boundary conditions. Section 2.1 introduces the notations and different opposite-edge-support conditions of the plate element. Section 2.2 and Section 2.3 exhibit the development of elemental DS formulations for inplane vibration and out-of-plane vibration, respectively. The assembly procedure of the elemental matrices is

shown in Section 2.4, and the algorithm of the DSM is improved in Section 2.5.

2.1. Different Boundary Conditions of a Plate Element.

Figure 1 shows a plate element with a pair of opposite edges supported. For notational convenience, the boundaries $y = 0$ and $y = L$ are denoted by supported boundaries (SBs), whereas the boundaries $x = 0$ and $x = b$ are represented by nodal boundaries (NBs), and the corresponding boundary conditions are abbreviated as SBC and NBC, respectively.

Table 1 lists the physical meanings of four types of SBCs, namely, S1 and S2 SBCs for inplane vibration (see Figure 2) and S and G for out-of-plane vibration (Figure 3), as well as all possible SBC combinations of a plate. More specifically, an S1 SBC along the edge (either $y = 0$ or $y = L$) means inplane vibration is constrained in the x direction but can move freely in the y direction; an S2 SBC means that the edge is fixed in the y direction but can move freely in the x direction.

It is known that existing dynamic stiffness formulations in the literature could have ten combinations of the NBCs for inplane and transverse vibrations, which are extended in

the current research for the NBCs for both inplane and transverse vibrations (see Table 2) to 40, respectively, in Table 2. This will no doubt broaden the application scope of the DSM. The letter "F" in Table 2 denotes a free edge and "C" indicates a clamped boundary. The sequence of the SBC combinations is supported boundary1-supported boundary2 and of NBC combinations is nodal boundary1-nodal boundary2.

Thus, the possible boundary conditions of a plate element considering both inplane and out-of-plane vibrations are increased from 100 (10×10) to 1600 (40×40), which greatly improves the engineering applicability of the DSM.

2.2. Dynamic Stiffness Formulation for Inplane Vibration of a Plate Element.

This section focuses on inplane vibration of plate elements with three different SBCs, as provided in Table 2, namely, S1-S1, S2-S2, and S1-S2 (it is easily seen that the DS formulation for a rectangular plate element with S2-S1 SBC should be similar to that with S1-S2 SBC and thus is omitted here for conciseness).

By using Hamilton's principle, the governing differential equation (GDE) in the time domain for the inplane free vibratory motion can be deduced as follows:

$$
\begin{cases}
\dfrac{Eh}{1-\nu^2}\left(\dfrac{\partial^2 u(x,y,t)}{\partial x^2} + \dfrac{1-\nu}{2}\dfrac{\partial^2 u(x,y,t)}{\partial y^2} + \dfrac{\nu+1}{2}\dfrac{\partial^2 v(x,y,t)}{\partial x \partial y}\right) - \rho h \dfrac{\partial^2 u(x,y,t)}{\partial t^2} = 0, \\[4mm]
\dfrac{Eh}{1-\nu^2}\left(\dfrac{\partial^2 v(x,y,t)}{\partial y^2} + \dfrac{1-\nu}{2}\dfrac{\partial^2 v(x,y,t)}{\partial x^2} + \dfrac{\nu+1}{2}\dfrac{\partial^2 u(x,y,t)}{\partial x \partial y}\right) - \rho h \dfrac{\partial^2 v(x,y,t)}{\partial t^2} = 0,
\end{cases}
\tag{1}
$$

which can be transferred into the frequency domain as

$$
\begin{cases}
\dfrac{\partial^2 U(x,y)}{\partial x^2} + \dfrac{1-\nu}{2}\dfrac{\partial^2 U(x,y)}{\partial y^2} + \dfrac{\nu+1}{2}\dfrac{\partial^2 V(x,y)}{\partial x \partial y} + \dfrac{1-\nu}{2Gh}\rho h \omega^2 U(x,y) = 0, \\[4mm]
\dfrac{\partial^2 V(x,y)}{\partial y^2} + \dfrac{1-\nu}{2}\dfrac{\partial^2 V(x,y)}{\partial x^2} + \dfrac{\nu+1}{2}\dfrac{\partial^2 U(x,y)}{\partial x \partial y} + \dfrac{1-\nu}{2Gh}\rho h \omega^2 V(x,y) = 0,
\end{cases}
\tag{2}
$$

and the natural BCs take the form

$$
\begin{cases}
\delta u: N_{xx} = \dfrac{2Gh}{1-\nu}\left(\dfrac{\partial u(x,y,t)}{\partial x} + \nu \dfrac{\partial v(x,y,t)}{\partial y}\right), \\[4mm]
\delta v: N_{xy} = Gh\left(\dfrac{\partial u(x,y,t)}{\partial y} + \dfrac{\partial v(x,y,t)}{\partial x}\right),
\end{cases}
\tag{3}
$$

where E is Young's modulus, h the thickness, ν the Poisson ratio, ρ the density, ω the angular frequency, and $G = (E/(2(1+\nu)))$ the shear modulus.

The triangles in Figure 2 indicate the boundary constraints of the inplane vibration. Based on Table 1, the

general solutions of equation (2) for inplane vibration with three different SBCs should take the following forms:

$$
\begin{cases}
U(x,y) = \begin{cases} \displaystyle\sum_{m=0}^{\infty} U_m(x)\sin(\alpha_m y), & \text{S1}-\text{S1 or S1}-\text{S2}, \\[4mm] \displaystyle\sum_{m=0}^{\infty} U_m(x)\cos(\alpha_m y), & \text{S2}-\text{S2}, \end{cases} \\[10mm]
V(x,y) = \begin{cases} \displaystyle\sum_{m=0}^{\infty} V_m(x)\cos(\alpha_m y), & \text{S1}-\text{S1 or S1}-\text{S2}, \\[4mm] \displaystyle\sum_{m=0}^{\infty} V_m(x)\sin(\alpha_m y), & \text{S2}-\text{S2}, \end{cases}
\end{cases}
\tag{4}
$$
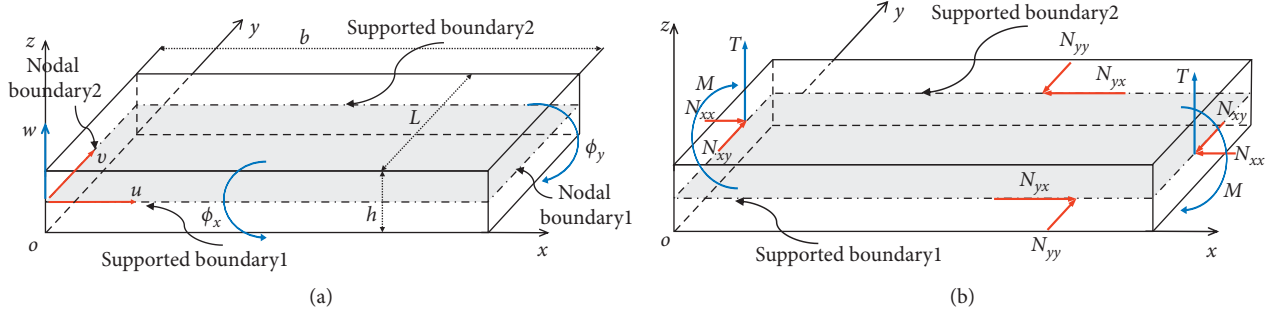
FIGURE 1: Coordinate system and notations for displacements (a) and forces (b).

TABLE 1: Physical meanings of all possible opposite-edge simple supports for a plate.

	SBC	$y = 0$ and $y = L$	$x = 0$ and $x = b$	Combinations
Inplane vibration	S1	$u = 0$ and $N_{yy} = 0$	$v = 0$ and $N_{xx} = 0$	S1-S1, S2-S2, S1-S2, S2-S1
	S2	$v = 0$ and $N_{yx} = 0$	$u = 0$ and $N_{xy} = 0$	
Out-of-plane vibration	S	$w = 0$ and $M = 0$	$w = 0$ and $M = 0$	S-S, G-G, S-G, G-S
	G	$\phi_x = 0$ and $T = 0$	$\phi_y = 0$ and $T = 0$	
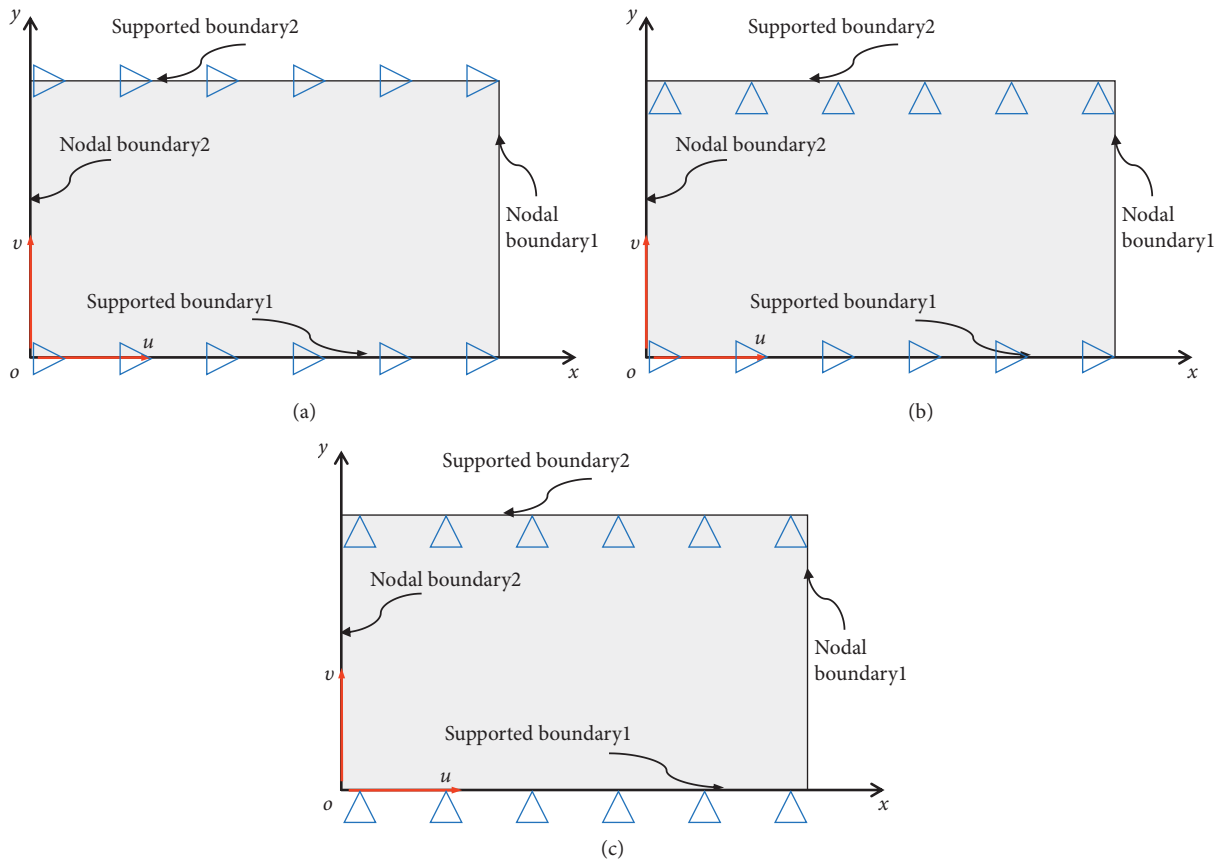
FIGURE 2: Three types of SBCs for inplane vibration: (a) S1-S1; (b) S1-S2; (c) S2-S2.
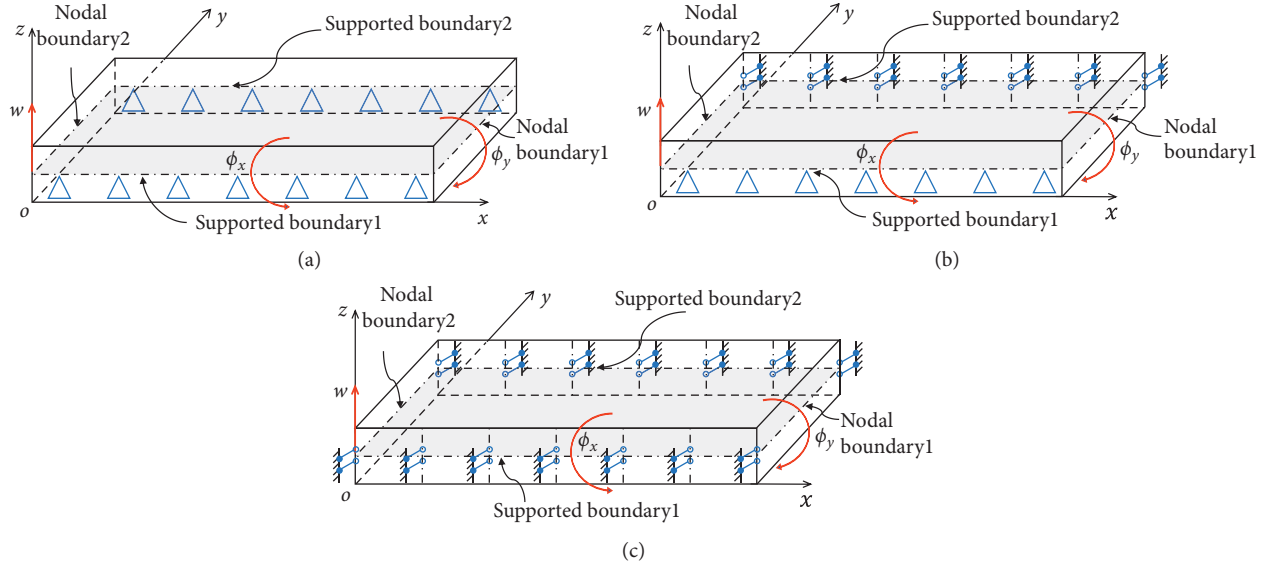
FIGURE 3: Three types of SBCs for out-of-plane vibration: (a) S-S; (b) S-G; (c) G-G.

TABLE 2: All possible BCs of a plate for inplane and out-of-plane vibrations.

	NBCs	SBCs	NBC no.
Inplane vibration	F-F, F-C, F-G, F-S, C-C, C-G, C-S, G-G, G-S, S-S	S-S	10
		S-G	10
		G-G	10
		G-S	10
Out-of-plane vibration	F-F, F-C, F-S2, F-S1, C-C, C-S2, C-S1, S2-S2, S2-S1, S1-S1	S1-S1	10
		S1-S2	10
		S2-S2	10
		S2-S1	10

with

$$\alpha_m = \begin{cases} \dfrac{m\pi}{L}, m = 0, 1, 2, \ldots, & \text{S1-S1 or S2-S2,} \\ \dfrac{(2m-1)\pi}{2L}, m = 1, 2, 3 \ldots, & \text{S1-S2,} \end{cases} \tag{5}$$

where the letter m stands for the half wave number of a plate element in the y direction and L is the length of the plate.

Substituting equation (4) into (2) leads to

$$\begin{cases} \dfrac{d^2 U_m(x)}{dx^2} - \left(a_1\alpha_m^2 - a_3\omega^2\right)U_m(x) \mp a_2\alpha_m\dfrac{dV_m(x)}{dx} = 0, \\ a_1\dfrac{d^2 V_m(x)}{dx^2} - \left(\alpha_m^2 - a_3\omega^2\right)V_m(x) \pm a_2\alpha_m\dfrac{dU_m(x)}{dx} = 0, \end{cases} \tag{6}$$

with

$$a_1 = \frac{1-\nu}{2},$$

$$a_2 = \frac{1+\nu}{2}, \tag{7}$$

$$a_3 = \frac{\rho\left(1-\nu^2\right)}{E},$$

where "$\mp$" and "$\pm$" take the first sign for S1-S1 and S1-S2 and the second sign for S2-S2, and they are the same in the remainder of Section 2.2.

By observing equation (6), it is necessary to divide it into two cases to solve the GDE: $m \neq 0$ and $m = 0$.

(1) $m \neq 0$. Substituting $U_m = e^{rx}$, $V_m = \delta e^{rx}$ into equation (6) leads to

$$\begin{cases} r^2 e^{rx} - \left(a_1\alpha_m^2 - a_3\omega^2\right)e^{rx} \mp a_2\alpha_m r\delta e^{rx} = 0, \\ a_1 r^2 \delta e^{rx} - \left(\alpha_m^2 - a_3\omega^2\right)\delta e^{rx} \pm a_2\alpha_m r e^{rx} = 0. \end{cases} \tag{8}$$

After some fundamental derivations, the exact general solution of equation (6) can be represented as follows:

$$\begin{cases} U_m(x) = A_{1m}\cosh\left(r_1 x\right) + A_{2m}\sinh\left(r_1 x\right) + A_{3m}\cosh\left(r_2 x\right) + A_{4m}\sinh\left(r_2 x\right), \\ V_m(x) = \mp\delta_1 A_{2m}\cosh\left(r_1 x\right) \mp \delta_1 A_{1m}\sinh\left(r_1 x\right) \mp \delta_2 A_{4m}\cosh\left(r_2 x\right) \mp \delta_2 A_{3m}\sinh\left(r_2 x\right), \end{cases} \tag{9}$$

where

$$r_{1,2} = \sqrt{\frac{2\alpha_m^2 E + (\nu - 3)(\nu + 1)\omega^2 \rho \pm \sqrt{(1+\nu)^4 \omega^4 \rho^2}}{2E}}, \quad (10)$$

$$\delta_i = \frac{a_1 \alpha_m^2 - a_3 \omega^2 - r_i^2}{a_2 \alpha_m r_i}, \quad i = 1, 2. \quad (11)$$

$$N_{xx_m}(x, y) = N_{xx_m}(x)\sin(\alpha_m y) = \frac{2Gh}{1-\nu} \begin{bmatrix} A_{1m}(r_1 + \nu\alpha_m \delta_1)\sinh(r_1 x) + A_{2m}(r_1 + \nu\alpha_m \delta_1)\cosh(r_1 x) \\ + A_{3m}(r_2 + \nu\alpha_m \delta_2)\sinh(r_2 x) + A_{4m}(r_2 + \nu\alpha_m \delta_2)\cosh(r_2 x) \end{bmatrix} \sin(\alpha_m y),$$

$$\quad (12)$$

$$N_{xy_m}(x, y) = N_{xy_m}(x)\cos(\alpha_m y) = \pm Gh \begin{bmatrix} A_{1m}(\alpha_m - \delta_1 r_1)\cosh(r_1 x) + A_{2m}(\alpha_m - \delta_1 r_1)\sinh(r_1 x) \\ + A_{3m}(\alpha_m - \delta_2 r_2)\cosh(r_2 x) + A_{4m}(\alpha_m - \delta_2 r_2)\sinh(r_2 x) \end{bmatrix} \cos(\alpha_m y).$$

When the SBC is S2-S2, $\sin(\alpha_m y)$ in equation (12) becomes $\cos(\alpha_m y)$, while $\cos(\alpha_m y)$ becomes $\sin(\alpha_m y)$.

The force and displacement NBCs of the plate element (Figure 4) are given as follows:

along $x = 0$, $U = U_1, V = V_1, N_{xx} = -N_{xx_1}, N_{xy} = -N_{xy_1}$,

along $x = b$, $U = U_2, V = V_2, N_{xx} = N_{xx_2}, N_{xy} = N_{xy_2}$.

$$\quad (13)$$

The relationship between the displacement NBCs and unknown coefficients is determined by applying the BCs for displacements to equation (9) as follows:

$$\{\mathbf{d}\} = \begin{Bmatrix} U_1 \\ V_1 \\ U_2 \\ V_2 \end{Bmatrix} = \begin{bmatrix} 1 & 0 & 1 & 0 \\ 0 & \mp\delta_1 & 0 & \mp\delta_2 \\ C_{h1} & S_{h1} & C_{h2} & S_{h2} \\ \mp\delta_1 S_{h1} & \mp\delta_1 C_{h1} & \mp\delta_2 S_{h2} & \mp\delta_2 C_{h2} \end{bmatrix} \begin{Bmatrix} A_1 \\ A_2 \\ A_3 \\ A_4 \end{Bmatrix}, \quad (14)$$

where $C_{hi} = \cosh(r_i b)$ and $S_{hi} = \sinh(r_i b)$.

Similarly, inserting force NBCs into equation (12) gives

$$\{\mathbf{f}\} = \begin{Bmatrix} N_{xx_1} \\ N_{xy_1} \\ N_{xx_2} \\ N_{xy_2} \end{Bmatrix} = Gh \begin{bmatrix} 0 & H_1 & 0 & H_2 \\ \mp P_1 & 0 & \mp P_2 & 0 \\ -H_1 S_{h1} & -H_1 C_{h1} & -H_2 S_{h2} & -H_2 C_{h2} \\ \pm P_1 C_{h1} & \pm P_1 S_{h1} & \pm P_2 C_{h2} & \pm P_2 S_{h2} \end{bmatrix} \begin{Bmatrix} A_1 \\ A_2 \\ A_3 \\ A_4 \end{Bmatrix}, \quad (15)$$

where $H_i = ((2(r_i + \alpha_m \delta_i \nu))/(\nu - 1))$ and $P_i = \alpha_m - \delta_i r_i$

By eliminating the coefficient vector of equations (14) and (15), the relationship between the force vector $\{\mathbf{f}\}$ and the displacement vector $\{\mathbf{d}\}$ can be written as $\{\mathbf{f}\} = [\mathbf{K}^i(\omega)]\{\mathbf{d}\}$; thus, the dynamic stiffness matrix for inplane vibration $[\mathbf{K}^i(\omega)]$ is derived as follows:

$$[\mathbf{K}^i(\omega)] = \frac{Gh}{\Delta^i} \begin{bmatrix} k_{11}^i & k_{12}^i & k_{13}^i & k_{14}^i \\ & k_{22}^i & -k_{14}^i & k_{24}^i \\ & & k_{11}^i & -k_{12}^i \\ Sym & & & k_{22}^i \end{bmatrix}, \quad (16)$$

By applying equation (9) to (3), the expressions of shear force and bending moment are determined as follows:
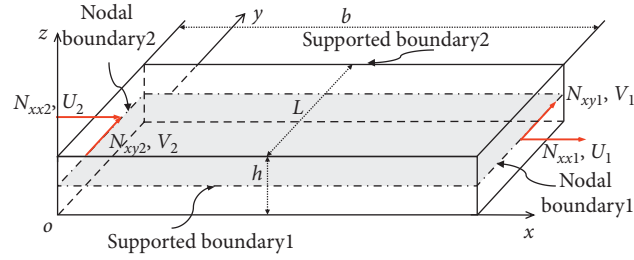
FIGURE 4: Force and displacement NBCs of a plate element.

where $[\mathbf{K}^i(\omega)]$ is a symmetric matrix, which is composed of 6 elements k_{11}^i, k_{12}^i, k_{13}^i, k_{14}^i, k_{22}^i, and k_{24}^i. The expressions of these 6 elements are as follows:

$$
\begin{aligned}
\Delta^i &= 2\delta_1\delta_2\left(1 - C_{h1}C_{h2}\right) + S_{h1}S_{h2}\left(\delta_1^2 + \delta_2^2\right), \\[6pt]
k_{11}^i &= \frac{2\left(r_2\delta_1 - r_1\delta_2\right)\left(C_{h1}S_{h2}\delta_2 - C_{h2}S_{h1}\delta_1\right)}{(\nu - 1)}, \\[6pt]
k_{12}^i &= \frac{\mp 2\left(\left(1 - C_{h1}C_{h2}\right)\left(r_2\delta_1 + \left(r_1 + 2\alpha_m\nu\delta_1\right)\delta_2\right) + S_{h1}S_{h2}\left(\delta_1\left(r_1 + \alpha_m\nu\delta_1\right) + \delta_2\left(r_2 + \alpha_m\nu\delta_2\right)\right)\right)}{(\nu - 1)}, \\[6pt]
k_{13}^i &= \frac{2\left(r_1\delta_2 - r_2\delta_1\right)\left(S_{h2}\delta_2 - S_{h1}\delta_1\right)}{(\nu - 1)}, \\[6pt]
k_{14}^i &= \frac{\mp 2\left(C_{h1} - C_{h2}\right)\left(r_1\delta_2 - r_2\delta_1\right)}{(\nu - 1)}, \\[6pt]
k_{22}^i &= \left(r_1\delta_1 - r_2\delta_2\right)\left(C_{h1}S_{h2}\delta_1 - C_{h2}S_{h1}\delta_2\right), \\[6pt]
k_{24}^i &= \left(r_2\delta_2 - r_1\delta_1\right)\left(S_{h2}\delta_1 - S_{h1}\delta_2\right).
\end{aligned}
\tag{17}
$$

(2) $m = 0$. From equation (4), it is easily seen that the solution procedure in the case of $m = 0$ is different from the case of $m \neq 0$ when the SBs of the plate are constrained by S1-S1 and S2-S2. For the sake of brevity, this paper only provides the detailed derivation when the SBC is S2-S2. A similar procedure can be performed when the SBC is S1-S1, but here we only include the final formulation.

It is obvious that the plate element can move in the direction of $U(x, y)$ with $U(x, y) = U_m(x)\cos(\alpha_m y)$ and the displacement of $V(x, y)$ is always equal to zero by applying $m = 0$ to equation (4). As a consequence, equation (6) can be simplified as

$$
\frac{d^2 U_m(x)}{dx^2} + a_3\omega^2 U_m(x) = 0,
\tag{18}
$$

where a_3 is given by equation (7). The general solution of equation (18) can be written in the form

$$
U_m(x) = A_1'\cos(rx) + A_2'\sin(rx),
\tag{19}
$$

with $r = \omega\sqrt{a_3}$.

The function for force of inplane vibration is defined by substituting equation (19) into (3) as follows:

$$
\begin{aligned}
N_{xx_m}(x, y) &= N_{xx_m}(x) \\[4pt]
&= \frac{Ehr}{1 - \nu^2}\left(-A_1'\sin(rx) + A_2'\cos(rx)\right).
\end{aligned}
\tag{20}
$$

The BCs in this case are given by

$$
\begin{aligned}
\text{at } x = 0, \quad & U = U_1, N_{xx} = -N_{xx_1}, \\
\text{at } x = b, \quad & U = U_2, N_{xx} = N_{xx_2}.
\end{aligned}
\tag{21}
$$

Applying the displacement NBCs of equation (21) to (19) leads to

$$
\left\{ \begin{matrix} U_1 \\ U_2 \end{matrix} \right\} = \left[\begin{matrix} 1 & 0 \\ C & S \end{matrix} \right] \left\{ \begin{matrix} A_1' \\ A_2' \end{matrix} \right\},
\tag{22}
$$

where $C = \cos(rb)$ and $S = \sin(rb)$.

Inserting the force NBCs of equation (21) to (20) gives

$$\begin{Bmatrix} N_{xx_1} \\ N_{xx_2} \end{Bmatrix} = \frac{Ehr}{1 - v^2} \begin{bmatrix} 0 & -1 \\ -S & C \end{bmatrix} \begin{Bmatrix} A_1' \\ A_2' \end{Bmatrix}. \tag{23}$$

The dynamic stiffness matrix for inplane vibration in this situation is resolved by eliminating the constants A_1' and A_2' of equations (22) and (23):

$$\left[\mathbf{K}^i (\omega) \right] = Ghr \begin{bmatrix} k_{11}'^i & k_{12}'^i \\ k_{12}'^i & k_{11}'^i \end{bmatrix}, \tag{24}$$

where the two elements of $[\mathbf{K}^i (\omega)]$ are exhibited as follows:

$$\begin{cases} k_{11}'^i = \dfrac{2}{1 - v} \cot(rb), \\[3mm] k_{12}'^i = \dfrac{-2}{1 - v} \csc(rb). \end{cases} \tag{25}$$

Similarly, when the SBC is S1-S1 and $m = 0$, $U(x, y)$ and force of $N_{xx}(x, y)$ are always equal to zero. In this case, the dynamic stiffness matrix takes a similar form of equation (24), whereas the entries are slightly different [34].

$$\begin{cases} k_{11}'^i = \cot(rb), \\[2mm] k_{12}'^i = -\csc(rb), \end{cases} \tag{26}$$

with $r = \omega \sqrt{(a_3/a_1)}$.

2.3. Dynamic Stiffness Formulation for Out-of-Plane Vibration of a Plate Element. In this section, the dynamic stiffness (DS) formulations are developed for the out-of-plane vibration of a plate element with three different SBCs, i.e., S-S, S-G, and G-G (it is easily seen that the DS formulation of the S-G SBC is the same as that of the G-S SBC for transverse free vibration of a rectangular plate element).

The DS matrix for out-of-plane vibration can be developed in a similar way as inplane vibration. Since the matrix for plate elements under the S-S SBC has been developed previously, e.g., by Boscolo and Banerjee [17], the expressions under the S-G and G-G SBCs are obtained in this study.

The GDE in the time domain of out-of-plane vibration is given by

$$D\left(\frac{\partial^4 w(x, y, t)}{\partial x^4} + 2 \frac{\partial^4 w(x, y, t)}{\partial x^2 \partial y^2} + \frac{\partial^4 w(x, y, t)}{\partial y^4} \right)$$
$$+ \rho h \frac{\partial^2 w(x, y, t)}{\partial t^2} = 0, \tag{27}$$

which can be transferred into the frequency domain as

$$\frac{\partial^4 W(x, y)}{\partial x^4} + 2 \frac{\partial^4 W(x, y)}{\partial x^2 \partial y^2} + \frac{\partial^4 W(x, y)}{\partial y^4} - \frac{\rho h \omega^2}{D} W(x, y) = 0. \tag{28}$$

The natural BCs take the form

$$\begin{cases} \delta w : V_x = -D\left(\dfrac{\partial^3 w(x, y, t)}{\partial x^3} + (2 - v) \dfrac{\partial^3 w(x, y, t)}{\partial x \partial y^2} \right), \\[4mm] \delta \phi_y : M_{xx} = -D\left(\dfrac{\partial^2 w(x, y, t)}{\partial x^2} + v \dfrac{\partial^2 w(x, y, t)}{\partial y^2} \right), \end{cases} \tag{29}$$

where $D = (Eh^3/(12(1 - v^2)))$ is the bending stiffness of the plate.

Figure 3 shows the boundary constraints of the transverse vibration. The general solutions of equation (28) with three different SBCs can be written as

$$W(x, y) = \begin{cases} \displaystyle\sum_{m=1}^{\infty} W_{mn}(x) \sin(\alpha_{om} y), & \text{S-S or S-G}, \\[4mm] \displaystyle\sum_{m=0}^{\infty} W_{mn}(x) \cos(\alpha_{om} y), & \text{G-G}, \end{cases} \tag{30}$$

with

$$\alpha_{om} = \begin{cases} \dfrac{m\pi}{L}, & m = 1, 2, 3 \ldots, \text{S-S}, \\[3mm] \dfrac{m\pi}{L}, & m = 0, 1, 2, \ldots, \text{G-G}, \\[3mm] \dfrac{(2m - 1)\pi}{2L}, & m = 1, 2, 3 \ldots, \text{S-G}. \end{cases} \tag{31}$$

Substituting equation (30) into (28) gives (except for the case of G-G with $m = 0$)

$$\frac{d^4 W_m(x)}{dx^4} - 2\alpha_{om}^2 \frac{d^2 W_m(x)}{dx^2} + \left(\alpha_{om}^4 - \frac{\rho h \omega^2}{D} \right) W_m(x) = 0. \tag{32}$$

In the case of the SBC being G-G, when $m = 0$, equation (32) becomes

$$\frac{d^4 W_m(x)}{dx^4} - \frac{\rho h \omega^2}{D} W_m(x) = 0. \tag{33}$$

It is found that the dynamic stiffness formulation for a plate element under the above two SBCs is very similar to the case under the S-S SBC. For the sake of completeness, the dynamic stiffness matrix is reported here as

$$[\mathbf{K}^o (\omega)] = \frac{D}{\Delta^o} \begin{bmatrix} k_{11}^o & k_{12}^o & k_{13}^o & k_{14}^o \\ & k_{22}^o & -k_{14}^o & k_{24}^o \\ & & k_{11}^o & -k_{12}^o \\ Sym & & & k_{22}^o \end{bmatrix}, \tag{34}$$

where $[\mathbf{K}^o (\omega)]$ is a symmetric matrix, which is composed of 6 elements k_{11}^o, k_{12}^o, k_{13}^o, k_{14}^o, k_{22}^o, and k_{24}^o; the expressions of these 6 elements are as follows:

$$\Delta^o = r_1^2 S_{h1} S_{h2} + r_2^2 S_{h1} S_{h2} + r_1 r_2 \left((C_{h1} - C_{h2})^2 - S_{h1}^2 - S_{h2}^2 \right),$$

$$k_{11}^o = (r_2 R_1 - r_1 R_2)(C_{h2} S_{h1} R_1 - C_{h1} S_{h2} R_2),$$

$$k_{12}^o = r_1 \left(R_2 (C_{h1} C_{h2} + S_{h1}^2 - C_{h1}^2) - R_1 S_{h1} S_{h2} \right)$$
$$+ r_2 \left(R_1 (C_{h1} C_{h2} + S_{h2}^2 - C_{h2}^2) - R_2 S_{h1} S_{h2} \right),$$

$$k_{13}^o = (L_2 - L_1)(r_2 C_{h2} S_{h1} - r_1 C_{h1} S_{h2}),$$

$$k_{14}^o = (r_2 R_1 - r_1 R_2)(r_2 S_{h2} - r_1 S_{h1}),$$

$$k_{22}^o = (C_{h2} - C_{h1})(r_2 R_1 - r_1 R_2),$$

$$k_{24}^o = (L_1 - L_2)(r_2 S_{h1} - r_1 S_{h2}),$$

$$(35)$$

where $r_i = \sqrt{\alpha_{om}^2 \pm \omega \sqrt{(\rho h / D)}}$ $(i = 1, 2)$, "$\pm$" takes the first sign for $i = 1$ and the second sign for $i = 2$, S_{hi} and C_{hi} are the same as in Section 2.2, $R_i = r_i^3 - \alpha_{om}^2 r_i (2 - \nu)$, and $L_i = r_i^2 - \alpha_{om}^2 \nu$.

2.4. Coordinate Transformation, Assembly Procedure, and Nodal Boundary Condition Applications.

As the dynamic stiffness formulations of inplane and out-of-plane vibrations are derived in the previous sections, the plate elements can be assembled to model plate built-up structures. In this section, a transformation matrix is developed to transform the elemental dynamic stiffness matrix from the local coordinate system to the global coordinate system. Then, all elemental dynamic stiffness matrices of plate elements are assembled directly to obtain a global dynamic stiffness matrix of the complex plate built-up structure, and any boundary conditions can be applied on the nodal boundaries. Finally, modal analysis is performed by using the Wittrick–Williams algorithm.

2.4.1. Coordinate Transformation.

Taking the structure in Figure 5 as an example, assuming that the coordinate system of plate 1 (P_1 of Figure 5) coincides with the global coordinate system, the displacement and force vectors of plate 2 (P_2 of Figure 5) need to be converted to the global coordinate system for the assembly purpose.

Supposing $\{U^l, V^l, W^l, \phi^l\}$ is the displacement vector of a nodal boundary in the local coordinate system of plate 2, when $m \neq 0$, the displacement vector in the global coordinate system $\{U^g, V^g, W^g, \phi^g\}$ is given by

$$\begin{Bmatrix} U^g \\ V^g \\ W^g \\ \phi^g \end{Bmatrix} = \begin{bmatrix} \cos(\theta) & 0 & \sin(\theta) & 0 \\ 0 & 1 & 0 & 0 \\ -\sin(\theta) & 0 & \cos(\theta) & 0 \\ 0 & 0 & 0 & 1 \end{bmatrix} \begin{Bmatrix} U^l \\ V^l \\ W^l \\ \phi^l \end{Bmatrix}. \quad (36)$$

The transformation matrix $\mathbf{T}$ of the displacement vector of a plate element can be written as

$$\mathbf{T} = \begin{bmatrix} \cos(\theta) & 0 & \sin(\theta) & 0 & 0 & 0 & 0 & 0 \\ 0 & 1 & 0 & 0 & 0 & 0 & 0 & 0 \\ -\sin(\theta) & 0 & \cos(\theta) & 0 & 0 & 0 & 0 & 0 \\ 0 & 0 & 0 & 1 & 0 & 0 & 0 & 0 \\ 0 & 0 & 0 & 0 & \cos(\theta) & 0 & \sin(\theta) & 0 \\ 0 & 0 & 0 & 0 & 0 & 1 & 0 & 0 \\ 0 & 0 & 0 & 0 & -\sin(\theta) & 0 & \cos(\theta) & 0 \\ 0 & 0 & 0 & 0 & 0 & 0 & 0 & 1 \end{bmatrix}. \quad (37)$$

It should be emphasized that, in the case of $m = 0$, the displacement of V^l is equal to 0 when the SBC is S2-S2; then, the displacement vector (U^g, W^g, ϕ^g) takes the form

$$\begin{Bmatrix} U^g \\ W^g \\ \phi^g \end{Bmatrix} = \begin{bmatrix} \cos(\theta) & \sin(\theta) & 0 \\ -\sin(\theta) & \cos(\theta) & 0 \\ 0 & 0 & 1 \end{bmatrix} \begin{Bmatrix} U^l \\ W^l \\ \phi^l \end{Bmatrix}. \quad (38)$$

In this case, $\mathbf{T}$ becomes

$$\mathbf{T} = \begin{bmatrix} \cos(\theta) & \sin(\theta) & 0 & 0 & 0 & 0 \\ -\sin(\theta) & \cos(\theta) & 0 & 0 & 0 & 0 \\ 0 & 0 & 1 & 0 & 0 & 0 \\ 0 & 0 & 0 & \cos(\theta) & \sin(\theta) & 0 \\ 0 & 0 & 0 & -\sin(\theta) & \cos(\theta) & 0 \\ 0 & 0 & 0 & 0 & 0 & 1 \end{bmatrix}. \quad (39)$$

Similarly, the transformation matrix $\mathbf{T}$ for the case of S1-S1 and $m = 0$ is

$$\mathbf{T} = \begin{bmatrix} 1 & 0 & 0 & 0 & 0 & 0 \\ 0 & \cos(\theta) & 0 & 0 & 0 & 0 \\ 0 & 0 & 1 & 0 & 0 & 0 \\ 0 & 0 & 0 & 1 & 0 & 0 \\ 0 & 0 & 0 & 0 & \cos(\theta) & 0 \\ 0 & 0 & 0 & 0 & 0 & 1 \end{bmatrix}. \quad (40)$$

The transformation matrix of the forces can also be defined using the same method, and it is exactly the transposed matrix of $\mathbf{T}$. Thus, the spatial transformation function of plate elements is given as follows:

$$\mathbf{K}_e^g = \mathbf{T}^T \mathbf{K}_e^l \mathbf{T}. \quad (41)$$

2.4.2. Assembly Procedure.

Once all degrees of freedom (DOFs) of plate elements have been transferred into the global coordinate system, the plate elements can be assembled. It should be noted that there are two types of boundaries, namely, nodal boundaries (NBs) and supported boundaries (SBs), and only NBs can be used for the nodal assembly. The procedure is similar to the finite element method. Take Figure 5 as an example, in which plate1 and plate2 share the same nodal boundary L_4. Equations (42) and (43) are the dynamic stiffness matrices of plate1 and plate2, respectively. Therefore, the assembly of plate1 and plate2 becomes a 12×12 matrix by summing the entries at the common nodal boundary L_4, namely,

FIGURE 5: A two-plate built-up structure.

$$
\left\{
\begin{array}{c}
N^1_{xx2} \\
N^1_{xy2} \\
T^1_2 \\
M^1_2 \\
N^1_{xx4} \\
N^1_{xy4} \\
T^1_4 \\
M^1_4
\end{array}
\right\}
=
\left[
\begin{array}{cccccccc}
\Delta & \Delta & \Delta & \Delta & \Delta & \Delta & \Delta & \Delta \\
\Delta & \Delta & \Delta & \Delta & \Delta & \Delta & \Delta & \Delta \\
\Delta & \Delta & \Delta & \Delta & \Delta & \Delta & \Delta & \Delta \\
\Delta & \Delta & \Delta & \Delta & \Delta & \Delta & \Delta & \Delta \\
\Delta & \Delta & \Delta & \Delta & \Delta & \Delta & \Delta & \Delta \\
\Delta & \Delta & \Delta & \Delta & \Delta & \Delta & \Delta & \Delta \\
\Delta & \Delta & \Delta & \Delta & \Delta & \Delta & \Delta & \Delta \\
\Delta & \Delta & \Delta & \Delta & \Delta & \Delta & \Delta & \Delta
\end{array}
\right]
\left\{
\begin{array}{c}
U^1_2 \\
V^1_2 \\
W^1_2 \\
\phi^1_2 \\
U^1_4 \\
V^1_4 \\
W^1_4 \\
\phi^1_4
\end{array}
\right\},
\tag{42}
$$

$$
\left\{
\begin{array}{c}
N^2_{xx4} \\
N^2_{xy4} \\
T^2_4 \\
M^2_4 \\
N^2_{xx6} \\
N^2_{xy6} \\
T^2_6 \\
M^2_6
\end{array}
\right\}
=
\left\{
\begin{array}{cccccccc}
\blacksquare & \blacksquare & \blacksquare & \blacksquare & \blacksquare & \blacksquare & \blacksquare & \blacksquare \\
\blacksquare & \blacksquare & \blacksquare & \blacksquare & \blacksquare & \blacksquare & \blacksquare & \blacksquare \\
\blacksquare & \blacksquare & \blacksquare & \blacksquare & \blacksquare & \blacksquare & \blacksquare & \blacksquare \\
\blacksquare & \blacksquare & \blacksquare & \blacksquare & \blacksquare & \blacksquare & \blacksquare & \blacksquare \\
\blacksquare & \blacksquare & \blacksquare & \blacksquare & \blacksquare & \blacksquare & \blacksquare & \blacksquare \\
\blacksquare & \blacksquare & \blacksquare & \blacksquare & \blacksquare & \blacksquare & \blacksquare & \blacksquare \\
\blacksquare & \blacksquare & \blacksquare & \blacksquare & \blacksquare & \blacksquare & \blacksquare & \blacksquare \\
\blacksquare & \blacksquare & \blacksquare & \blacksquare & \blacksquare & \blacksquare & \blacksquare & \blacksquare
\end{array}
\right\}
\left\{
\begin{array}{c}
U^2_4 \\
V^2_4 \\
W^2_4 \\
\phi^2_4 \\
U^2_6 \\
V^2_6 \\
W^2_6 \\
\phi^2_6
\end{array}
\right\},
\tag{43}
$$

$$
\left\{
\begin{array}{c}
N_x \\
N_{xy2} \\
T_2 \\
M_2 \\
N_{xx4} \\
N_{xy4} \\
T_4 \\
M_4 \\
N_{xx6} \\
N_{xy6} \\
T_6 \\
M_6
\end{array}
\right\}
=
\left\{
\begin{array}{cccccccccccc}
\Delta & \Delta & \Delta & \Delta & \Delta & \Delta & \Delta & \Delta & 0 & 0 & 0 & 0 \\
\Delta & \Delta & \Delta & \Delta & \Delta & \Delta & \Delta & \Delta & 0 & 0 & 0 & 0 \\
\Delta & \Delta & \Delta & \Delta & \Delta & \Delta & \Delta & \Delta & 0 & 0 & 0 & 0 \\
\Delta & \Delta & \Delta & \Delta & \Delta & \Delta & \Delta & \Delta & 0 & 0 & 0 & 0 \\
\Delta & \Delta & \Delta & \Delta & (\Delta+\blacksquare) & (\Delta+\blacksquare) & (\Delta+\blacksquare) & (\Delta+\blacksquare) & \blacksquare & \blacksquare & \blacksquare & \blacksquare \\
\Delta & \Delta & \Delta & \Delta & (\Delta+\blacksquare) & (\Delta+\blacksquare) & (\Delta+\blacksquare) & (\Delta+\blacksquare) & \blacksquare & \blacksquare & \blacksquare & \blacksquare \\
\Delta & \Delta & \Delta & \Delta & (\Delta+\blacksquare) & (\Delta+\blacksquare) & (\Delta+\blacksquare) & (\Delta+\blacksquare) & \blacksquare & \blacksquare & \blacksquare & \blacksquare \\
\Delta & \Delta & \Delta & \Delta & (\Delta+\blacksquare) & (\Delta+\blacksquare) & (\Delta+\blacksquare) & (\Delta+\blacksquare) & \blacksquare & \blacksquare & \blacksquare & \blacksquare \\
0 & 0 & 0 & 0 & \blacksquare & \blacksquare & \blacksquare & \blacksquare & \blacksquare & \blacksquare & \blacksquare & \blacksquare \\
0 & 0 & 0 & 0 & \blacksquare & \blacksquare & \blacksquare & \blacksquare & \blacksquare & \blacksquare & \blacksquare & \blacksquare \\
0 & 0 & 0 & 0 & \blacksquare & \blacksquare & \blacksquare & \blacksquare & \blacksquare & \blacksquare & \blacksquare & \blacksquare \\
0 & 0 & 0 & 0 & \blacksquare & \blacksquare & \blacksquare & \blacksquare & \blacksquare & \blacksquare & \blacksquare & \blacksquare
\end{array}
\right\}
\left\{
\begin{array}{c}
U_2 \\
V_2 \\
W_2 \\
\phi_2 \\
U_4 \\
V_4 \\
W_4 \\
\phi_4 \\
U_6 \\
V_6 \\
W_6 \\
\phi_6
\end{array}
\right\}.
\tag{44}
$$

2.4.3. Application of Nodal Boundary Conditions.

In this research, SBs denote a pair of boundaries in which any combinations of simply supported and/or guided supports can be applied, and any arbitrary classical BCs can be applied to the NBs by deleting the certain columns and rows for corresponding fixed DOFs in equation (44). For example, when L_2 and L_4 are free with L_6 fully clamped, the last 4 values in the displacement vector of equation (44) are zero. Then, the global dynamic stiffness matrix of the structure in Figure 5 can be written as

$$
\left[\mathbf{K}^g_{\text{FFC}}\right] =
\begin{bmatrix}
\Delta & \Delta & \Delta & \Delta & \Delta & \Delta & \Delta & \Delta \\
\Delta & \Delta & \Delta & \Delta & \Delta & \Delta & \Delta & \Delta \\
\Delta & \Delta & \Delta & \Delta & \Delta & \Delta & \Delta & \Delta \\
\Delta & \Delta & \Delta & \Delta & \Delta & \Delta & \Delta & \Delta \\
\Delta & \Delta & \Delta & \Delta & (\Delta+\blacksquare) & (\Delta+\blacksquare) & (\Delta+\blacksquare) & (\Delta+\blacksquare) \\
\Delta & \Delta & \Delta & \Delta & (\Delta+\blacksquare) & (\Delta+\blacksquare) & (\Delta+\blacksquare) & (\Delta+\blacksquare) \\
\Delta & \Delta & \Delta & \Delta & (\Delta+\blacksquare) & (\Delta+\blacksquare) & (\Delta+\blacksquare) & (\Delta+\blacksquare) \\
\Delta & \Delta & \Delta & \Delta & (\Delta+\blacksquare) & (\Delta+\blacksquare) & (\Delta+\blacksquare) & (\Delta+\blacksquare)
\end{bmatrix}.
\tag{45}
$$

By the similar way, various complex plate built-up structures can be assembled in this research.

2.5. Wittrick–William Algorithm and J_0 Counts.

Once the dynamic stiffness matrix is developed, the Wittrick–Williams algorithm can be applied to compute the natural frequencies ω of structures. The following equation is the key equation of the Wittrick–Williams algorithm, which is used to calculate the mode count J when ω is lower than the trial frequency ω^*:

$$
J = J_0 + s\left\{\left[\mathbf{K}(\omega^*)\right]\right\},
\tag{46}
$$

where $\left[\mathbf{K}(\omega^*)\right]$ is the elemental dynamic stiffness matrix when $\omega = \omega^*$, $s\{[\mathbf{K}(\omega^*)]\}$ is the number of negative diagonal elements after upper triangular transformation by using Gauss elimination of $[\mathbf{K}(\omega^*)]$, and J_0 is the number of natural frequencies between $\omega = 0$ and $\omega = \omega^*$ when the nodal boundaries (NBs) of the plate element are fully clamped.

There is no doubt that J_0 plays an important role in the Wittrick–Williams algorithm. However, calculating J_0 is generally a difficult problem, and the traditional way is to refine the mesh to make sure $J_0 = 0$ [17, 34–36]. Obviously, it will introduce unnecessary computational cost significantly.

In this study, the J_0 problem of the plate element is resolved by applying an indirect method; it improves the computational efficiency of the dynamic stiffness method. According to the Wittrick–Williams algorithm, the mode count J_{sm} of the plate element with all NBs simply supported (or guided) when the half wave number in the y direction is m can be given by equation (46), which can be recast as

$$
J_{0m} = J_{sm} - s\left\{\left[\mathbf{K}^s_m(\omega^*)\right]\right\},
\tag{47}
$$

where J_{0m} is J_0 when the half wave number in the y direction is m and $[\mathbf{K}^s_m(\omega^*)]$ is the dynamic stiffness matrix $[\mathbf{K}(\omega^*)]$ for a plate element with all NBs simply supported (or guided) when m is a certain value. The analytical expression for J_{sm} is given as follows: the first step is to establish the relationship between m, n, and ω, where n is the half wave number in the x direction.

2.5.1. J_0 Formulations for Inplane Vibration.

Consider the BC of the plate element is S1S1S1S1, then the general solution of equation (2) for inplane vibration should take the following form:

$$
\begin{cases}
U(x, y) = \displaystyle\sum_{m=1}^{\infty}\sum_{n=1}^{\infty} U_{mn}\sin(\alpha_m y)\cos\left(\dfrac{n\pi}{b}x\right), \\[2mm]
V(x, y) = \displaystyle\sum_{m=0}^{\infty}\sum_{n=0}^{\infty} V_{mn}\cos(\alpha_m y)\sin\left(\dfrac{n\pi}{b}x\right).
\end{cases}
\tag{48}
$$

Substituting equation (48) into (2), the relationship between m, n, and ω under the S1-S1 or S2-S2 SBC is determined by

$$
\left(\frac{1-\nu}{2}\right)^2\beta^4 - \frac{(1-\nu)(3-\nu)}{4}\left(\frac{m^2\pi^2}{L^2} + \frac{n^2\pi^2}{b^2}\right)\beta^2
$$
$$
+ \frac{1-\nu}{2}\left(\frac{m^2\pi^2}{L^2} + \frac{n^2\pi^2}{b^2}\right)^2 = 0,
\tag{49}
$$

where $\beta = \omega\sqrt{(\rho/G)}$ and b is the width of the plate.

Solving equation (49) gives

$$
\Gamma \geq n^2 + (\eta m)^2,
\tag{50}
$$

$$
\Gamma \geq \frac{2\times\left(n^2 + (\eta m)^2\right)}{1-\nu},
\tag{51}
$$

with

$$
\eta = \frac{b}{L},
$$
$$
\Gamma = \left(\frac{b\beta}{\pi}\right)^2.
\tag{52}
$$

Suppose J^i_{sm} is J_{sm} for inplane vibration of a fully simply supported plate. Therefore, J^i_{sm} consists of two parts which can be solved from equations (50) and (51) separately.
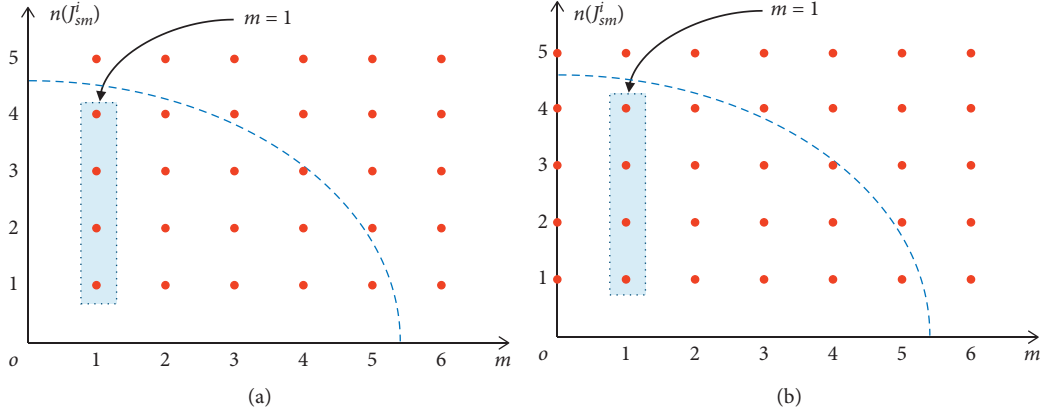
Equation (50) can be expressed in the form

$$
n^2 + (\eta m)^2 - \Gamma \leq 0.
\tag{53}
$$

So, natural modes exist for all integers $m, n \geq 1$, as shown in Figure 6. Essentially, J^i_{sm1} is the mode count of an S2S2S2S2 or S1S1S2S1 plate when m is fixed which is obtained by solving n of equation (53):

$$
J^i_{sm1} = \text{floor}\left(\sqrt{\Gamma - (\eta m)^2}\right),
\tag{54}
$$

where $\text{floor}(x)$ indicates the largest integer not greater than x.

FIGURE 6: J_{sm1}^i of S2S2S2S2 (a) and S1S1S2S1 (b).

For an S1S1S1S1 plate, natural modes exist for all $m, n \geq 0$ except for $m = n = 0$ (Figure 7). Thus, J_{sm1}^i of S1S1S1S1 takes the form

$$J_{sm1}^i = \mathrm{ceil}\left(\sqrt{\Gamma - (\eta m)^2} \right), \qquad (55)$$

where $\mathrm{ceil}(x)$ is the least integer not less than x. It should be emphasized that m in equation (54) becomes $((2m + 1)/2)$ for $m = 0, 1, 2 \ldots$, when the BC is S1S1S2S1.

Similar to equation (50), equation (51) can be written as

$$\frac{2}{1 - \nu}\left(n^2 + (\eta m)^2\right) - \Gamma \leq 0. \qquad (56)$$

When the BC is S2S2S2S2, $m, n \geq 0$ except $m = n = 0$ (Figure 8). By solving equation (56), J_{sm2}^i of S2S2S2S2 is given by

$$J_{sm2}^i = \mathrm{ceil}\left(\sqrt{\frac{(1 - \nu)\Gamma}{2} - (\eta m)^2} \right). \qquad (57)$$

In Figure 9, when the BC is S1S1S1S1 or S1S1S2S1, for $m, n \geq 1$, J_{sm2}^i becomes

$$J_{sm2}^i = \mathrm{floor}\left(\sqrt{\frac{(1 - \nu)\Gamma}{2} - (\eta m)^2} \right). \qquad (58)$$

In particular, when the BC is S1S1S2S1, m is replaced by $((2m + 1)/2), m = 0, 1, 2 \ldots$.
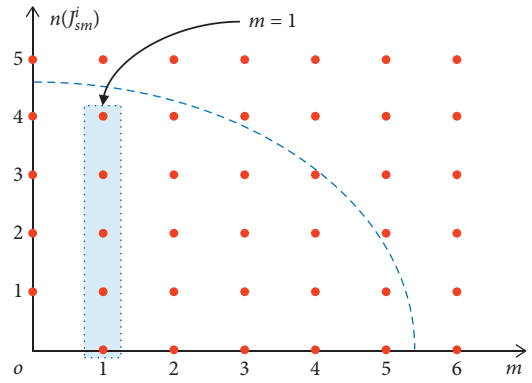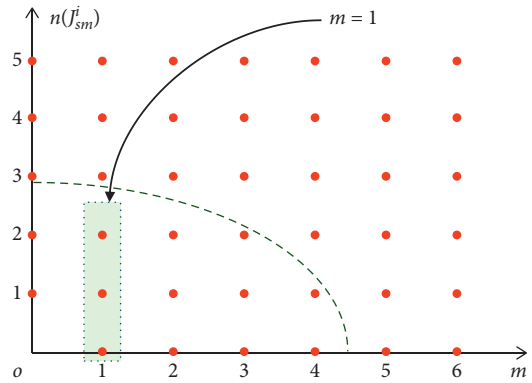
Adding J_{sm1}^i and J_{sm2}^i together gives

$$J_{sm}^i = J_{sm1}^i + J_{sm2}^i. \qquad (59)$$

FIGURE 7: J_{sm1}^i of S1S1S1S1.

FIGURE 8: J_{sm2}^i of S2S2S2S2.

2.5.2. J_0 Formulations for Transverse Free Vibration.
Similar to Section 2.5.1, J_0 of out-of-plane vibration is derived by an indirect method as well.

Consider the BC of the plate element is SSSS, then the general solution of equation (28) for out-of-plane vibration should take the following form:

$$W(x, y) = \sum_{m=1}^{\infty} \sum_{n=1}^{\infty} W_{mn} \sin(\alpha_{om} y) \sin\left(\frac{n\pi}{b} x\right). \qquad (60)$$

Substituting equation (60) into (28), the relationship between m, n, and ω under the S-S SBC and S-S NBC is determined by

$$\omega_{mn}^2 = \frac{D}{\rho h} \frac{\pi^4}{L^4} \left(\left(\frac{L}{b}\right)^4 n^4 + 2\left(\frac{L}{b}\right)^2 M^2 n^2 + M^4 \right), \qquad (61)$$

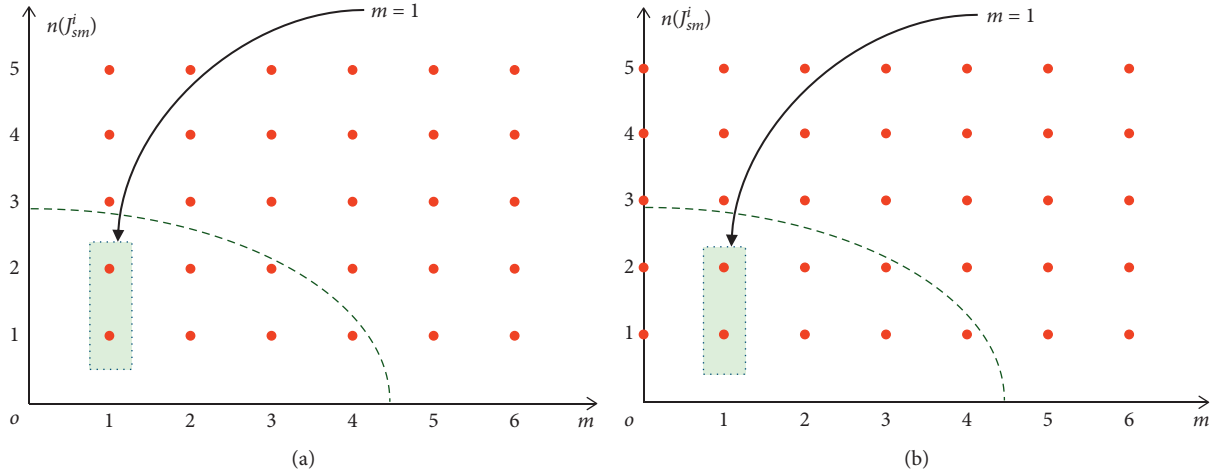which is also valid for G-G and S-G SBCs with the S-S NBC with

FIGURE 9: J_{sm2}^{i} of S1S1S1S1 (a) and S1S1S2S1 (b).

$$M = \begin{cases} m, m = 1, 2, 3 \ldots, & \text{S-S,} \\ m, m = 0, 1, 2, \ldots, & \text{G-G,} \\ \dfrac{2m-1}{2}, m = 1, 2, 3, \ldots, & \text{S-G.} \end{cases} \quad (62)$$

Suppose J_{sm}^{o} is J_{sm} for out-of-plane vibration of the fully simply supported (or guided) plate and the half wave number in the y direction is m. By solving equation (61), one can solve J_{sm}^{o} as

$$J_{sm}^{o} = \text{floor}\left(\frac{b}{\pi}\sqrt{\omega\sqrt{\frac{\rho h}{D}} - \alpha_{om}^{2}}\right) + i_{\text{SG}}, \quad (63)$$

with

$$i_{\text{SG}} = \begin{cases} 0, & \text{S} - \text{S or S} - \text{G,} \\ 1, & \text{G} - \text{G.} \end{cases} \quad (64)$$

3. Results

An efficient program for exact modal analysis of individual plates and complex plate built-up structures was compiled in MATLAB based on the dynamic stiffness method described in Section 2. Section 3.1 demonstrates the application of the DSM (Section 2.3) to the out-of-plane free vibration of an individual plate with a comprehensive combination of boundary conditions. Section 3.2 applies the DSM (Section 2.2) to the inplane modal analysis of a single plate under different boundary conditions. Section 3.3 computes the natural modes of three plate built-up structures by the DSM, including a two-plate built-up structure (Section 3.3.1), an I-shaped plate built-up structure (Section 3.3.2), and a section of an extruded aluminum panel (Section 3.3.3), and compares the DSM with the FEM. All DSM and FEM computations are performed on the same computer with an 8 GB Intel Core i5-7200U processor.

3.1. Modal Analysis of Out-of-Plane Vibration for an Individual Plate.
Table 3 exhibits the first 8 natural frequencies of the out-of-plane vibration for a square plate ($E = 72$ GPa, $\nu = 0.3$, $\rho = 2800\,\text{kg}\cdot\text{m}^{-3}$, $h = 0.002\,\text{m}$, and $L = b = 1\,\text{m}$) calculated by the DSM under three different BCs, namely, S-F-S-F, S-F-G-F, and G-F-G-F. The BCs are listed in order of bottom, right, up, and left in an anticlockwise sense. The results are compared with FEM results with different element sizes (0.1×0.1, 0.05×0.05, and 0.01×0.01) by using SHELL181 elements in ANSYS.

It can be seen from Table 3 that as the element size becomes smaller, the FEM results converge to the DSM results. When the size is 0.01×0.01, the differences of the first 8 natural frequencies between the DSM and the FEM are within ±0.1%. It is worth noting that, in this case, the FEM uses 10,000 elements for a total of 61,206 DOFs for calculation, while only 1 element with 4 DOFs is used for the DSM. It takes 2 seconds for the FEM (mesh size 0.01) to compute the first 10 modes of the individual plate under the S-F-S-F BC, while the DSM only costs 0.14 seconds. It is obvious that the DSM gives exact results with much higher computational efficiency than the FEM. Then, the first 8 natural frequencies of the plate under 27 classical BCs in Table 2 are shown in Table 4.

3.2. Modal Analysis of Inplane Vibration for an Individual Plate.
The first 8 natural frequencies of inplane vibration for an individual plate (Table 5) are calculated by using the DSM and FEM under three representative BCs, namely, S1-F-S1-F, S1-F-S2-F, and S2-F-S2-F. The structure is the same as in Section 3.1, while only the inplane motion is considered in this section. The results in Table 5 show that the FEM results converge to the DSM results as the FEM mesh becomes refined from size = 0.1 to size = 0.01, and in the case of size = 0.01, the FEM spends 3 seconds, while the DSM only costs 0.08 seconds to compute the same modes of the individual plate under the S1-F-S1-F BC. It is clear that the DSM is a more efficient and accurate method of inplane vibration analysis than the FEM. The relative errors between

Table 3: Natural frequencies (ω, rad·s^{-1}) of a square plate under out-of-plane vibration by using the DSM and FEM. The FEM results are calculated in ANSYS by using 3 different element sizes (0.1×0.1, 0.05×0.05, and 0.01×0.01) of SHELL181 elements.

Mode	DSM	FEM (relative error (%))		
		Size = 0.1	Size = 0.05	Size = 0.01
S-F-S-F				
1	29.5593	29.9318 (1.26)	29.6516 (0.31)	29.5624 (0.01)
2	49.5187	49.8420 (0.65)	49.5970 (0.16)	49.5084 (−0.02)
3	112.713	113.996 (1.14)	113.035 (0.28)	112.695 (−0.02)
4	119.525	125.708 (5.17)	121.020 (1.25)	119.575 (0.04)
5	143.442	149.075 (3.93)	144.809 (0.95)	143.470 (0.02)
6	217.106	223.204 (2.81)	218.611 (0.69)	217.103 (0.00)
7	231.050	241.532 (4.54)	233.678 (1.14)	231.108 (0.03)
8	270.037	303.032 (12.22)	277.723 (2.85)	270.315 (0.10)
S-F-G-F				
1	7.29859	7.32117 (0.31)	7.30420 (0.08)	7.29855 (0.00)
2	21.1168	21.1404 (0.11)	21.1216 (0.02)	21.1121 (−0.02)
3	66.9707	68.8888 (2.86)	67.4437 (0.71)	66.9850 (0.02)
4	80.9386	81.9516 (1.25)	81.1913 (0.31)	80.9400 (0.00)
5	89.6413	91.3387 (1.89)	90.0569 (0.46)	89.6422 (0.00)
6	158.503	161.070 (1.62)	159.147 (0.41)	158.493 (−0.01)
7	187.214	202.670 (8.26)	190.896 (1.97)	187.346 (0.07)
8	200.157	210.901 (5.37)	202.828 (1.33)	200.245 (0.04)
G-F-G-F				
1	29.5593	29.9318 (1.26)	29.6516 (0.31)	29.5624 (0.01)
2	49.5187	49.8433 (0.66)	49.5988 (0.16)	49.5172 (0.00)
3	68.6650	69.7057 (1.52)	68.9265 (0.38)	68.6752 (0.01)
4	112.713	114.002 (1.14)	113.041 (0.29)	112.714 (0.00)
5	119.525	125.708 (5.17)	121.020 (1.25)	119.582 (0.05)
6	143.442	149.081 (3.93)	144.809 (0.95)	143.483 (0.03)
7	189.278	200.258 (5.80)	192.002 (1.44)	189.382 (0.05)
8	217.106	223.204 (2.81)	218.617 (0.70)	217.134 (0.01)

Table 4: The first 8 natural frequencies (ω, rad·s^{-1}) of out-of-plane vibration for an individual square plate under 27 classical BCs. All parameters are the same as in Table 3.

BCs	1	2	3	4	5	6	7	8
S-F-S-F	29.5593	49.5187	112.713	119.525	143.442	217.106	231.050	270.037
S-F-S-C	38.9383	101.479	127.986	193.397	222.193	278.092	316.610	343.417
S-F-S-G	29.8811	54.2765	120.271	130.081	147.213	228.724	264.820	271.193
S-F-S-S	35.8606	85.1860	126.435	181.276	189.854	277.118	289.977	334.278
S-C-S-C	88.8520	168.010	212.769	290.288	313.708	396.202	430.297	475.017
S-C-S-G	42.0025	118.754	130.701	203.476	256.231	281.446	340.694	350.978
S-C-S-S	72.5721	158.592	179.989	264.352	307.734	347.504	410.613	432.264
S-G-S-G	30.2904	60.5809	121.162	151.452	151.452	242.324	272.614	302.905
S-G-S-S	37.8631	98.4439	128.734	189.315	219.606	280.187	310.477	340.768
S-S-S-S	60.5809	151.452	151.452	242.324	302.905	302.905	393.776	393.776
S-F-G-F	7.29859	21.1168	66.9707	80.9386	89.6413	158.503	187.214	200.157
S-F-G-C	17.5055	75.7883	76.5541	140.425	195.438	197.653	260.940	262.096
S-F-G-G	7.38983	28.1783	67.5092	93.6371	102.587	172.450	188.166	215.513
S-F-G-S	12.3797	57.7624	73.6886	126.366	162.739	194.231	232.694	250.455
S-C-G-C	73.0917	119.967	194.991	232.763	244.068	352.266	377.279	410.467
S-C-G-G	22.2130	78.4270	99.0506	153.308	198.425	235.793	269.398	291.000
S-C-G-S	53.1923	107.574	159.892	214.567	225.389	326.790	329.678	382.508
S-G-G-G	7.57261	37.8631	68.1535	98.4439	128.734	189.315	189.315	219.606
S-G-G-S	15.1452	75.7261	75.7261	136.307	196.888	196.888	257.469	257.469
G-F-G-F	29.5593	49.5187	68.6650	112.713	119.525	143.442	189.278	217.106
G-F-G-C	10.7909	38.9383	67.6253	101.479	127.986	189.353	193.397	222.193
G-F-G-G	17.1663	29.8811	54.2765	92.7651	120.271	130.081	147.213	228.724
G-F-G-S	35.8606	47.3195	85.1860	126.435	153.345	181.276	189.854	277.118
G-C-G-C	68.6650	88.8520	168.010	189.278	212.769	290.288	313.708	371.060
G-C-G-G	17.1663	42.0025	92.7651	118.754	130.701	203.476	229.072	256.231
G-C-G-S	47.3195	72.5721	153.345	158.592	179.989	264.352	307.734	319.943
G-G-G-G	30.2904	30.2904	60.5809	121.162	121.162	151.452	151.452	242.324

Table 5: Natural frequencies (ω, rad·s^{-1}) of the plate for inplane vibration analysis using the DSM and FEM. All parameters are the same as in Table 3.

Mode	DSM	FEM (relative error (%))		
		Size = 0.1	Size = 0.05	Size = 0.01
S1-F-S1-F				
1	7482.01	7560.56 (1.05)	7501.49 (0.26)	7482.65 (0.01)
2	9879.85	9961.99 (0.83)	9900.42 (0.21)	9880.94 (0.01)
3	13972.2	14091.3 (0.85)	14001.5 (0.21)	13973.2 (0.01)
4	17268.5	17944.1 (3.91)	17432.7 (0.95)	17275.0 (0.04)
5	17881.5	18078.6 (1.10)	17930.3 (0.27)	17883.2 (0.01)
6	18598.5	18814.4 (1.16)	18652.3 (0.29)	18600.7 (0.01)
7	19759.7	20351.2 (2.99)	19924.0 (0.83)	19766.3 (0.03)
8	19841.5	20436.7 (3.00)	19964.8 (0.62)	19846.7 (0.03)
S1-F-S2-F				
1	2732.44	2735.32 (0.11)	2733.19 (0.03)	2732.49 (0.00)
2	7869.56	7886.65 (0.22)	7874.09 (0.06)	7869.69 (0.00)
3	12405.5	12689.5 (2.29)	12475.3 (0.56)	12408.0 (0.02)
4	12991.5	13081.6 (0.69)	13013.7 (0.17)	12992.4 (0.01)
5	15875.7	16080.6 (1.29)	15926.6 (0.32)	15877.6 (0.01)
6	16674.7	16890.5 (1.29)	16727.7 (0.32)	16676.8 (0.01)
7	22053.0	22909.1 (3.88)	22368.8 (1.43)	22065.3 (0.06)
8	22306.7	23377.8 (4.80)	22452.3 (0.65)	22312.2 (0.02)
S2-F-S2-F				
1	7482.01	7560.56 (1.05)	7501.49 (0.26)	7482.64 (0.01)
2	13972.2	14091.3 (0.85)	14001.5 (0.21)	13973.2 (0.01)
3	16700.0	16838.9 (0.83)	16734.6 (0.21)	16701.3 (0.01)
4	17268.5	17944.1 (3.91)	17432.1 (0.95)	17275.0 (0.04)
5	17881.5	18078.6 (1.10)	17930.3 (0.27)	17883.2 (0.01)
6	18598.5	18814.4 (1.16)	18652.3 (0.29)	18600.7 (0.01)
7	19841.5	20351.2 (2.57)	19964.8 (0.62)	19846.7 (0.03)
8	26764.4	27484.5 (2.69)	26941.0 (0.66)	26771.4 (0.03)

the DSM and the FEM are within 0.06% when the element size of FEM is 0.01×0.01. Compared with out-of-plane vibration, the DSM and FEM agree better in inplane vibration analysis. It is because the DSM and FEM are based on the same governing differential equation in inplane vibration analysis. Table 6 provides the first 8 natural frequencies of the plate computed by the DSM under 27 classical BCs in Table 2. It is clear that the BCs have a great influence on the natural frequencies of inplane vibration for the plate.

3.3. Modal Analysis of Plate Built-Up Structures.

In this section, free vibration analysis by using the DS formulations developed in this paper on three plate built-up structures in engineering applications is performed, namely, a two-plate built-up structure (Section 3.3.1), an I-shaped plate built-up structure (Section 3.3.2), and a section of an extruded aluminum panel (Section 3.3.3).

3.3.1. A Two-Plate Built-Up Structure.

Consider a two-plate built-up structure with two plates connecting at an angle of θ (Figure 5), then the geometry and material properties of the 2 plates are the same ($E = 72$ GPa, $\nu = 0.3$, $\rho = 2700$ kg·m^{-3}, $L = 3$ m, $b = 2$ m, and $h = 0.02$ m). The SBs are L_1, L_5, L_3, and L_7, where the BCs of L_1 and L_5 should be the same and those of L_3 and L_7 are the same. Therefore, there are 16

(4×4) kinds of SBCs of the plate built-up structure, as shown in Table 7. The SBCs are listed in order of L_1 (L_5)-L_3 (L_7).

Firstly, the influences of angles on the natural frequencies of the two-plate built-up structure are tabulated in Table 8. The BCs of this plate built-up structure in Table 8 are listed in an anticlockwise sense of L_1 − $L_2 - L_3 - L_3 - L_4 - L_5 - L_6 - L_7$. Table 8 lists the first 8 natural frequencies of the two-plate built-up structure with two plates connecting at angles of 30, 60, 90, 120, 150, and 180° under (S1 G)-F-(S1 G)-F-(S1 G)-F-(S1 G) BCs. It can be found from Table 8 that the connection angles have little effect on the natural frequencies except for 180°. In order to explain this phenomenon, this study computed the first 8 natural frequencies of the structure at different angles under the 10 different SBCs in Table 7 with free nodal boundaries. Here are the conclusions: the natural frequencies of the structure at the angle of 180° are significantly different from those of other angles (the differences are much greater than 2%). The rates of change are less than 2% when the structure is at different angles (except 180°) under the SBCs of (S1 S)-(S1 S), (S1 S)-(S1 G), and (S1 G)-(S1 G), and part of the rates are more than 2% under the SBCs of (S1 S)-(S2 S), (S1 G)-(S2 S), (S1 S)-(S2 G), (S1 G)-(S2 G), (S2 S)-(S2 S), (S2 S)-(S2 G), and (S2 G)-(S2 G). It might be due to the reason that the BCs along the opposite sides of the two-plate built-up structure are simply supported (or guided), the two plates are weakly coupled, and the low-frequency modes are mainly dominated by out-of-plane vibration. Therefore, the angles (except 180°) have little effect on the first 30 natural frequencies of the structure in this section. When these two plates are connected at an angle of 180°, the transverse and inplane vibrations are fully coupled.

Then, Table 9 shows the influence of SBCs on the first 8 natural frequencies of the two-plate built-up structure with two plates connecting at an angle of 60°. The BCs of the plate built-up structure in Table 9 are listed in the order of $L_1 - L_5 - L_3 - L_7$, and the NBCs are free. It can be found that the natural frequencies of the structure have little differences when the SBCs related to out-of-plane vibration are the same although the SBCs for inplane vibration are different. This is due to the same reason as in Table 8: low-frequency modes are mainly dominated by out-of-plane vibration. Thus, the SBCs related to out-of-plane vibration have dominant influence on the low natural frequencies.

All the results of the DSM and FEM match well with each other, as shown in Tables 8 and 9 (differences within 1%). In this section, only 2 elements with 12 DOFs are adopted for the DSM, whereas the FEM uses as much as 30,000 elements (the element size is 0.02×0.02) and 182,106 DOFs to compute the results in Tables 8 and 9. It is obvious that the dynamic stiffness method has incomparable advantages in modal analysis of plate built-up structures.

3.3.2. I-Shaped Plate Built-Up Structure.

Now we consider an I-shaped plate built-up structure ($E = 72$ GPa, $\nu = 0.3$, $\rho = 2700$ kg · m^{-3}, $L = 3$ m, $b = 1$ m, $\Delta z = 2$ m, and $h = 0.01$ m), as shown in Figure 10, and the material and

Table 6: The first 8 natural frequencies (ω, rad·s^{-1}) of inplane vibration for an individual plate under 27 classical BCs.

BCs	1	2	3	4	5	6	7	8
S1-F-S1-F	7482.01	9879.85	13972.2	17268.5	17881.5	18598.5	19759.7	19841.5
S1-F-S1-C	4939.93	10512.0	14819.8	16274.3	18281.3	22126.5	23713.7	24699.6
S1-F-S1-S2	9879.85	9920.77	16263.1	18197.1	18207.1	19759.7	22636.4	24499.0
S1-F-S1-S1	4939.93	8634.27	13972.2	14819.8	18024.8	18334.7	21462.3	22887.6
S1-C-S1-C	9879.85	17410.3	18576.7	19759.7	23445.5	26351.6	29639.6	29880.9
S1-C-S1-S2	4939.93	14819.8	14940.4	18341.5	22669.5	23002.0	24699.6	27269.8
S1-C-S1-S1	9879.85	11722.7	18190.3	19759.7	20547.6	22544.6	25649.3	28966.7
S1-S2-S1-S2	9879.85	13972.2	16700.0	19759.7	22092.0	22092.0	23617.4	27944.4
S1-S2-S1-S1	4939.93	11046.0	14819.8	17811.2	18671.2	20367.8	24699.6	24699.6
S1-S1-S1-S1	9879.85	9879.85	13972.2	19759.7	19759.7	22092.0	22092.0	23617.4
S1-F-S2-F	2732.44	7869.56	12405.5	12991.5	15875.7	16674.7	22053.0	22306.7
S1-F-S2-C	8496.99	9353.77	14086.9	17210.7	21926.0	22691.3	23326.0	27186.5
S1-F-S2-S2	6986.11	8940.77	13382.2	13856.7	20205.3	20958.3	22661.5	25006.1
S1-F-S2-S1	3741.00	9299.24	13384.8	14757.2	17459.9	19068.9	22600.7	24085.0
S1-C-S2-C	12683.7	16429.9	19933.7	21967.8	24894.1	27510.3	29457.6	31443.9
S1-C-S2-S2	9288.33	14960.9	18673.3	18979.4	24888.1	25239.7	26998.2	27195.8
S1-C-S2-S1	8705.15	13175.8	15941.6	20249.4	22076.1	25302.5	26285.1	27578.2
S1-S2-S2-S2	8350.00	11046.0	17811.2	18671.2	20367.8	24699.6	25050.0	26602.3
S1-S2-S2-S1	6986.11	11808.7	15621.4	15621.4	20958.3	25188.8	25188.8	26405.0
S2-F-S2-F	7482.01	13972.2	16700.0	17268.5	17881.5	18598.5	19841.5	26764.4
S2-F-S2-C	8350.00	10512.0	16274.3	18281.3	22126.5	23713.7	25050.0	25565.0
S2-F-S2-S2	8350.00	9920.77	16263.1	18197.1	18207.1	22636.4	24499.0	25050.0
S2-F-S2-S1	8634.3	13972.2	16700.0	18024.8	18334.7	21462.3	22887.6	27145.9
S2-C-S2-C	16700.0	17410.3	18576.7	23445.5	26351.6	29880.9	29921.8	31883.1
S2-C-S2-S2	14940.4	16700.0	18341.5	22669.5	23002.0	27269.8	29047.9	31526.6
S2-C-S2-S1	8350.00	11722.7	18190.3	20547.6	22544.6	25050.0	25649.3	28966.7
S2-S2-S2-S2	13972.2	16700.0	16700.0	22092.0	22092.0	23617.4	27944.4	31242.8

Table 7: Different SBCs of a two-plate built-up structure.

IV	S1-S1	S1-S2	S2-S2	S2-S1
CPT	S-S	S-G	G-G	G-S

Table 8: The first 8 natural frequencies (ω, rad·s^{-1}) of the two-plate built-up structure with two plates connecting at different angles under (S1 G)-F-(S1 G)-F-(S1 G)-F-(S1 G) BCs (RE is short for relative error).

θ (°)		1	2	3	4	5	6	7	8
30	DSM	27.472	47.614	58.418	120.47	151.31	157.32	166.19	172.17
	FEM	27.470	47.540	58.359	120.22	151.14	157.20	165.77	172.10
	RE (%)	−0.01	−0.15	−0.10	−0.21	−0.11	−0.08	−0.25	−0.04
60	DSM	27.472	47.614	58.418	120.47	151.31	157.32	166.19	172.17
	FEM	27.469	47.547	58.359	120.40	151.17	157.20	165.89	172.07
	RE (%)	−0.01	−0.14	−0.10	−0.05	−0.09	−0.08	−0.18	−0.05
90	DSM	27.472	47.614	58.418	120.47	151.31	157.32	166.19	172.17
	FEM	27.469	47.549	58.358	120.44	151.18	157.19	165.91	172.01
	RE (%)	−0.01	−0.14	−0.10	−0.03	−0.09	−0.08	−0.17	−0.09
120	DSM	27.473	47.614	58.418	120.47	151.31	157.32	166.19	172.17
	FEM	27.466	47.551	58.354	120.45	151.19	157.17	165.93	171.83
	RE (%)	−0.02	−0.13	−0.11	−0.02	−0.08	−0.09	−0.16	−0.20
150	DSM	27.474	47.614	58.418	120.47	151.31	157.32	166.19	172.17
	FEM	27.453	47.559	58.332	120.45	151.20	157.09	165.95	170.83
	RE (%)	−0.08	−0.11	−0.15	−0.01	−0.07	−0.15	−0.15	−0.78
180	DSM	33.616	43.703	47.614	90.260	120.47	135.66	151.31	166.19
	FEM	33.612	43.701	47.579	90.151	120.45	135.62	151.22	166.00
	RE (%)	−0.01	−0.01	−0.07	−0.12	−0.01	−0.03	−0.06	−0.11

TABLE 9: The first 8 natural frequencies (ω, rad·s^{-1}) of the two-plate built-up structure with two plates connecting at an angle of 60° under different SBC combinations.

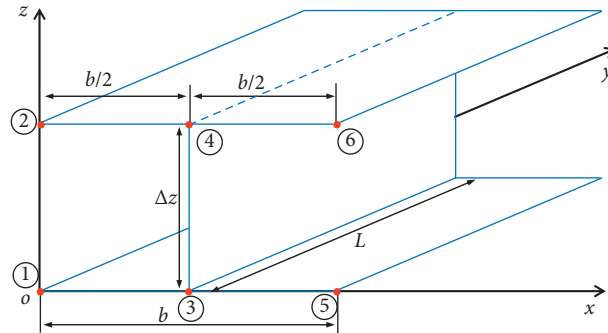| SBCs		1	2	3	4	5	6	7	8
	DSM	47.614	58.418	151.31	157.32	166.19	211.89	282.95	320.55
(S1 S)-(S1 S)-(S1 S)-(S1 S)	FEM	47.472	58.276	151.08	157.09	165.62	211.39	281.79	319.49
	RE (%)	−0.30	−0.24	−0.15	−0.14	−0.34	−0.24	−0.41	−0.33
	DSM	18.769	34.930	91.297	99.132	132.64	182.41	216.87	228.12
(S1 S)-(S1 S)-(S1 G)-(S1 G)	FEM	18.709	34.883	91.156	98.992	132.46	182.23	216.17	227.88
	RE (%)	−0.32	−0.13	−0.15	−0.14	−0.14	−0.10	−0.32	−0.11
	DSM	27.472	47.614	58.418	120.47	151.31	157.32	166.19	172.17
(S1 G)-(S1 G)-(S1 G)-(S1 G)	FEM	27.469	47.547	58.359	120.40	151.17	157.20	165.89	172.07
	RE (%)	−0.01	−0.14	−0.10	−0.05	−0.09	−0.08	−0.18	−0.05
	DSM	47.614	58.418	151.31	157.32	166.19	211.89	282.95	320.55
(S1 S)-(S1 S)-(S2 S)-(S2 S)	FEM	47.468	58.270	151.08	157.09	165.51	211.26	281.74	319.45
	RE (%)	−0.31	−0.25	−0.15	−0.15	−0.41	−0.30	−0.43	−0.34
	DSM	18.769	34.930	91.297	99.132	132.64	182.41	216.87	228.12
(S1 S)-(S1 S)-(S2 G)-(S2 G)	FEM	18.706	34.875	91.156	98.992	132.14	181.90	216.17	227.88
	RE (%)	−0.34	−0.16	−0.15	−0.14	−0.37	−0.28	−0.33	−0.11
	DSM	27.473	47.614	58.418	120.47	151.31	157.32	166.19	172.17
(S1 G)-(S1 G)-(S2 G)-(S2 G)	FEM	27.469	47.544	58.357	120.30	151.17	157.20	165.82	172.01
	RE (%)	−0.01	−0.15	−0.11	−0.14	−0.09	−0.08	−0.22	−0.09
	DSM	47.614	58.418	151.31	157.32	166.19	211.89	282.95	320.55
(S2 S)-(S2 S)-(S2 S)-(S2 S)	FEM	47.460	58.257	151.07	157.09	165.29	210.97	281.73	319.46
	RE (%)	−0.32	−0.28	−0.16	−0.15	−0.54	−0.44	−0.43	−0.34

FIGURE 10: I-shaped plate built-up structure.

TABLE 10: The first 8 natural frequencies (ω, rad·s^{-1}) of the I-shaped plate built-up structure under three representative SBCs. $E = 72$ GPa, $\nu = 0.3$, $\rho = 2700$ kg·m^{-3}, $L = 3$ m, $b = 1$ m, $\Delta z = 0.2$ m, and $h = 0.01$ m.

SBCs		1	2	3	4	5	6	7	8
	DSM	32.016	59.626	79.283	106.44	116.73	127.10	144.20	172.84
(S1 G)-(S1 G)	FEM	32.011	59.556	79.275	106.30	116.62	127.01	144.09	172.50
	RE (%)	−0.02	−0.12	−0.01	−0.13	−0.09	−0.08	−0.08	−0.19
	DSM	40.350	85.128	86.563	131.30	135.77	155.44	166.31	217.16
(S1 S)-(S2 G)	FEM	40.198	84.999	86.507	129.89	135.47	155.31	166.02	216.63
	RE (%)	−0.38	−0.15	−0.06	−1.07	−0.22	−0.08	−0.17	−0.24
	DSM	59.626	106.44	116.73	144.20	172.84	197.58	202.07	234.47
(S2 S)-(S2 S)	FEM	59.495	106.24	116.55	143.99	172.35	197.08	201.89	232.69
	RE (%)	−0.22	−0.19	−0.15	−0.15	−0.29	−0.25	−0.09	−0.76

thickness of all the plates are the same as in the previous example. There are 10 SBs on the side of $y = 0$ (front) and $y = L$ (back). The BCs of the SBs on the same side should be the same. Three representative SBCs of (S1 G)-(S1 G), (S1 S)-(S2 G), and (S2 S)-(S2 S) are considered for modal analysis.

Table 10 shows the comparisons of the results computed by the DSM and FEM. Only 5 dynamic stiffness elements with 24 DOFs are used for the I-shaped plate built-up structure, whereas the FEM uses 120,000 elements (the element size is 0.01×0.01) with a total of 724,206 DOFs. The
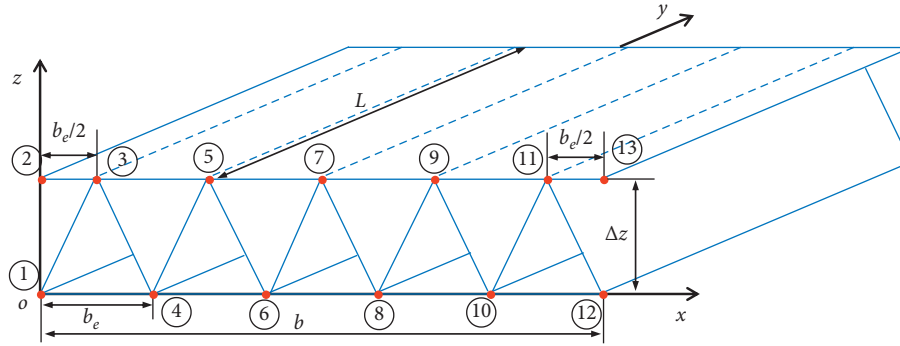
FIGURE 11: A section of an extruded aluminum panel.

TABLE 11: The first 8 natural frequencies (ω, rad·s^{-1}) of the extruded aluminum panel under three representative SBC combinations. $E = 72$ GPa, $\nu = 0.3$, $\rho = 2700$ kg·m^{-3}, $L = 0.2$ m, $b_e = 0.1$ m, $b = 0.5$ m, $\Delta z = 0.1$ m, and $h = 0.002$ m.

SBCs		1	2	3	4	5	6	7	8
(S1 G)-(S1 G)	DSM	2761.7	2764.6	3462.0	3552.8	3558.0	3558.8	3651.5	3864.5
	FEM	2763.1	2763.2	3470.0	3554.2	3555.0	3560.3	3657.9	3868.7
	RE (%)	0.05	−0.05	0.23	0.04	−0.09	0.04	0.18	0.11
(S1 S)-(S2 G)	DSM	2963.3	2966.4	3626.0	3717.2	3806.0	4010.9	4122.3	4475.2
	FEM	2957.4	2957.7	3630.6	3717.7	3807.9	3997.2	4105.9	4456.2
	RE (%)	−0.20	−0.29	0.13	0.01	0.05	−0.34	−0.40	−0.42
(S2 S)-(S2 S)	DSM	3558.0	3558.8	4131.0	4222.7	4285.0	4465.2	4591.9	4920.4
	FEM	3546.2	3546.9	4131.1	4220.1	4283.4	4448.8	4576.9	4906.5
	RE (%)	−0.33	−0.33	0.00	−0.06	−0.04	−0.37	−0.33	−0.28

(a)   (b)
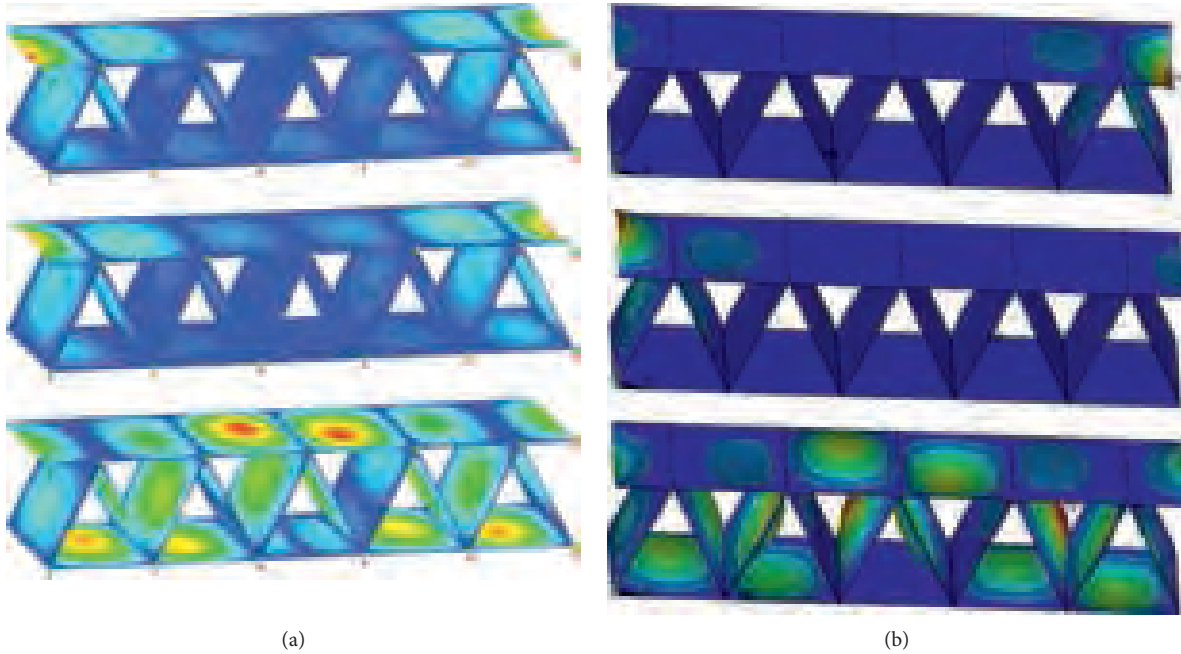
FIGURE 12: The first 3 modal shapes of the extruded aluminum panel computed by the DSM (a) and FEM (b).

DSM gives exact results, while the computational cost is extremely inexpensive.

3.3.3. A Section of an Extruded Aluminum Panel. Figure 11 shows a section of an extruded aluminum panel which has wide engineering applications such as the airplane fuselage and high-speed train body structures. In this section, the modal analysis of the structure in Figure 1 ($E = 72$ GPa, $\nu = 0.3$, $\rho = 2700$ kg·m^{-3}, $L = 0.2$ m, $b_e = 0.1$ m, $b = 0.5$ m, $\Delta z = 0.1$ m, and $h = 0.002$ m) is carried out by using the DSM and FEM under three different SBCs, and the material and thickness of all the plates are the same. Some representative natural frequencies are shown in Table 11 and

TABLE 12: Representative natural frequencies covering the whole frequency range of the first 100 natural frequencies (ω, rad·s^{-1}) of the I-shaped plate built-up structure and extruded aluminum panel in Figures 10 and 11 under the SBC combination of (S2 S)-(S2 S).

		10	30	50	70	90	100
	DSM	250.24	575.30	1008.3	1302.5	1563.8	1771.4
I-shaped plate built-up structure	FEM	249.61	574.35	1005.2	1295.1	1591.0	1767.8
	RE (%)	−0.25	−0.16	−0.31	−0.57	1.74	−0.21
	DSM	5403.4	7288.5	10458	14332	16015	16882
Extruded aluminum panel	FEM	5369.2	7262.1	10447	14323	16052	16926
	RE (%)	−0.63	−0.36	−0.10	−0.07	0.23	0.26

modal shapes in Figure 12. The DSM uses 21 elements with 52 DOFs to obtain the results, while 16,800 elements (the element size is 0.005 × 0.005) for a total of 101,352 DOFs are required for the FEM. It can be concluded that the results computed by the DSM and FEM agree well. Obviously, the DSM is applicable to the complex plate built-up structures, and therefore, the DSM is suitable for optimization design and parameter analysis due to its high efficiency and analytical nature.

Another advantage of the DSM for vibration analysis lies in its high efficiency and accuracy over the whole frequency range. Some representative natural frequencies covering the midfrequency and high-frequency ranges (10–100th modes) of the I-shaped plate built-up structure and extruded aluminum panel are listed in Table 12, where the SBC is (S2 S)-(S2 S). It is found that the computational efficiency of the DSM is more than 100 times that of the FEM. For example, the FEM takes 662 seconds to compute the first 100 modes of the I-shaped plate built-up structure, while the DSM only takes 3.28 seconds.

4. Conclusions

This paper has developed new formulations for both dynamic stiffness modelling and the associated algorithm for complex plate built-up structures for more general cases. In terms of modelling, dynamic stiffness formulations for plate elements with four different types of opposite-edge-support conditions and arbitrarily supported boundary conditions along other edges have been developed for both inplane and out-of-plane vibrations. As a result, the present formulations cover 16 types of opposite-edge-support boundary conditions (SBCs) with inplane and out-of-plane vibrations coupled, which is in a sharp contrast to existing research applicable to only one type of SBC and has greatly expanded the application range of the DSM. In terms of the algorithm, analytical expressions of the J_0 count for all SBCs discussed above have been developed for the Wittrick–Williams algorithm. With the J_0 problem resolved, there is no need to split a large dynamic stiffness element into smaller ones unnecessarily as the majority of existing works did. Therefore, very few DOFs are required for modelling complex plate built-up structures, which has made the DSM to be highly efficient for the whole frequency range. An efficient and accurate program has been developed based on the DS model for individual plates and plate built-up structures. The program has been applied to a couple of complex plate built-up structures in engineering applications, and exact natural frequencies and mode shapes within the whole frequency range are computed extremely efficiently.

This study focuses on the free vibration analysis of the structures; however, the formulations can also be used directly for forced vibration analysis, or extended to compute accurate key parameters for other methods. For example, it can compute the modal density and coupling loss factor which are key parameters for the statistical energy analysis (SEA) method especially within the midfrequency range. A drawback of the present study lies in that there are some limitations for opposite-edge-support conditions and the elements can only be assembled in one direction. In order to address these limitations, the spectral dynamic stiffness method [33, 38] can be used as a powerful alternative, but it will involve more degrees of freedom for more complex boundary conditions.

Data Availability

The data used to support the findings of this study are included within the article.

Conflicts of Interest

The authors declare that they have no conflicts of interest.

Acknowledgments

References

[1] L. Ji, X. Sheng, X. Xiao, Z. Wen, and X. Jin, "A review of midfrequency vibro-acoustic modelling for high-speed train extruded aluminium panels as well as the most recent developments in hybrid modelling techniques," *Journal of Modern Transportation*, vol. 23, no. 3, pp. 159–168, 2015.

[2] W. H. Wittrick and F. W. Williams, "A general algorithm for computing natural frequencies of elastic structures," *The Quarterly Journal of Mechanics and Applied Mathematics*, vol. 24, no. 3, pp. 263–284, 1971.

[3] V. Koloušek, "Anwendung des Gesetzes der virtuellen Verschiebungen und des Reziprozitätssatzes in der Stabwerksdynamik," *Ingenieur-Archiv*, vol. 12, no. 6, pp. 363–370, 1941.

[4] J. R. Banerjee and F. W. Williams, "Exact Bernoulli-Euler static stiffness matrix for a range of tapered beam-columns," *International Journal for Numerical Methods in Engineering*, vol. 23, no. 9, pp. 1615–1628, 1986.

[5] J. R. Banerjee and S. A. Fisher, "Coupled bending-torsional dynamic stiffness matrix for axially loaded beam elements," *International Journal for Numerical Methods in Engineering*, vol. 33, no. 4, pp. 739–751, 1992.

[6] J. R. Banerjee and F. W. Williams, "Coupled bending-torsional dynamic stiffness matrix for timoshenko beam elements," *Computers & Structures*, vol. 42, no. 3, pp. 301–310, 1992.

[7] J. R. Banerjee and F. W. Williams, "Coupled bending-torsional dynamic stiffness matrix of an axially loaded timoshenko beam element," *International Journal of Solids and Structures*, vol. 31, no. 6, pp. 749–762, 1994.

[8] J. R. Banerjee and A. J. Sobey, "Dynamic stiffness formulation and free vibration analysis of a three-layered sandwich beam," *International Journal of Solids and Structures*, vol. 42, no. 8, pp. 2181–2197, 2005.

[9] J. R. Banerjee and W. D. Gunawardana, "Dynamic stiffness matrix development and free vibration analysis of a moving beam," *Journal of Sound and Vibration*, vol. 303, no. 1-2, pp. 135–143, 2007.

[10] W. H. Wittrick and F. W. Williams, "Buckling and vibration of anisotropic or isotropic plate assemblies under combined loadings," *International Journal of Mechanical Sciences*, vol. 16, no. 4, pp. 209–239, 1974.

[11] M. S. Anderson, F. W. Williams, and C. J. Wright, "Buckling and vibration of any prismatic assembly of shear and compression loaded anisotropic plates with an arbitrary supporting structure," *International Journal of Mechanical Sciences*, vol. 25, no. 8, pp. 585–596, 1983.

[12] F. W. Williams and W. H. Wittrick, "An automatic computational procedure for calculating natural frequencies of skeletal structures," *International Journal of Mechanical Sciences*, vol. 12, no. 9, pp. 781–791, 1970.

[13] F. W. Williams, D. Kennedy, R. Butler, and M. S. Anderson, "VICONOPT-program for exact vibration and buckling analysis or design of prismatic plate assemblies," *AIAA Journal*, vol. 29, no. 11, pp. 1927-1928, 1991.

[14] F. W. Williams and J. R. Banerjee, "Accurately computed modal densities for panels and cylinders, including corrugations and stiffeners," *Journal of Sound and Vibration*, vol. 93, no. 4, pp. 481–488, 1984.

[15] A. N. Bercin, "An assessment of the effects of in-plane vibrations on the energy flow between coupled plates," *Journal of Sound and Vibration*, vol. 191, no. 5, pp. 661–680, 1996.

[16] A. N. Bercin and R. S. Langley, "Application of the dynamic stiffness technique to the in-plane vibrations of plate structures," *Computers & Structures*, vol. 59, no. 5, pp. 869–875, 1996.

[17] M. Boscolo and J. R. Banerjee, "Dynamic stiffness elements and their applications for plates using first order shear deformation theory," *Computers & Structures*, vol. 89, no. 3-4, pp. 395–410, 2011.

[18] W. Wu, X. Yin, H. Li, and K. Zhong, "Power flow analysis of built-up plate structures using the dynamic stiffness method," *Journal of Vibration and Control*, vol. 24, no. 13, pp. 2815–2831, 2018.

[19] X. Yin, W. Wu, K. Zhong, and H. Li, "Dynamic stiffness formulation for the vibrations of stiffened plate structures with consideration of in-plane deformation," *Journal of Vibration and Control*, vol. 24, no. 20, pp. 4825–4838, 2018.

[20] H. Li, X. Yin, and W. Wu, "Dynamic stiffness formulation for in-plane and bending vibrations of plates with two opposite edges simply supported," *Journal of Vibration and Control*, vol. 24, no. 9, pp. 1652–1669, 2016.

[21] A. W. Leissa and Y. Narita, "Vibrations of completely free shallow shells of rectangular planform," *Journal of Sound and Vibration*, vol. 96, no. 2, pp. 207–218, 1984.

[22] X. Liu and J. R. Banerjee, "Free vibration analysis for plates with arbitrary boundary conditions using a novel spectral-dynamic stiffness method," *Computers & Structures*, vol. 164, pp. 108–126, 2016.

[23] D. J. Gorman, "Accurate free vibration analysis of clamped orthotropic plates by the method of superposition," *Journal of Sound and Vibration*, vol. 140, no. 3, pp. 391–411, 1990.

[24] D. J. Gorman and W. Ding, "Accurate free vibration analysis of completely free symmetric cross-ply rectangular laminated plates," *Composite Structures*, vol. 60, no. 3, pp. 359–365, 2003.

[25] D. J. Gorman, "Accurate free vibration analysis of the completely free orthotropic rectangular plate by the method of superposition," *Journal of Sound and Vibration*, vol. 165, no. 3, pp. 409–420, 1993.

[26] D. J. Gorman, "Free vibration analysis of the completely free rectangular plate by the method of superposition," *Journal of Sound and Vibration*, vol. 57, no. 3, pp. 437–447, 1978.

[27] D. J. Gorman and S. D. Yu, "A review of the superposition method for computing free vibration eigenvalues of elastic structures," *Computers & Structures*, vol. 104-105, pp. 27–37, 2012.

[28] D. J. Gorman, "Exact solutions for the free in-plane vibration of rectangular plates with two opposite edges simply supported," *Journal of Sound and Vibration*, vol. 294, no. 1-2, pp. 131–161, 2006.

[29] Y. F. Xing and B. Liu, "Exact solutions for the free in-plane vibrations of rectangular plates," *International Journal of Mechanical Sciences*, vol. 51, no. 3, pp. 246–255, 2009.

[30] B. Liu and Y. Xing, "Exact solutions for free in-plane vibrations of rectangular plates," *Acta Mechanica Solida Sinica*, vol. 24, no. 6, pp. 556–567, 2011.

[31] Y. F. Xing and T. F. Xu, "Solution methods of exact solutions for free vibration of rectangular orthotropic thin plates with classical boundary conditions," *Composite Structures*, vol. 104, pp. 187–195, 2013.

[32] B. Liu and Y. Xing, "Comprehensive exact solutions for free in-plane vibrations of orthotropic rectangular plates," *European Journal of Mechanics-A/Solids*, vol. 30, no. 3, pp. 383–395, 2011.

[33] X. Liu and J. R. Banerjee, "An exact spectral-dynamic stiffness method for free flexural vibration analysis of orthotropic composite plate assemblies-part I: theory," *Composite Structures*, vol. 132, no. 15, pp. 1274–1287, 2015.

[34] M. Boscolo and J. R. Banerjee, "Dynamic stiffness method for exact inplane free vibration analysis of plates and plate assemblies," *Journal of Sound and Vibration*, vol. 330, no. 12, pp. 2928–2936, 2011.

[35] F. A. Fazzolari, J. R. Banerjee, and M. Boscolo, "Buckling of composite plate assemblies using higher order shear

deformation theory-An exact method of solution," *Thin-Walled Structures*, vol. 71, pp. 18–34, 2013.

[36] F. A. Fazzolari, M. Boscolo, and J. R. Banerjee, "An exact dynamic stiffness element using a higher order shear deformation theory for free vibration analysis of composite plate assemblies," *Composite Structures*, vol. 96, pp. 262–278, 2013.

[37] K. M. Ahmida and J. R. F. Arruda, "Estimation of the SEA coupling loss factors by means of spectral element modeling," *Journal of the Brazilian Society of Mechanical Sciences and Engineering*, vol. 25, no. 3, pp. 259–263, 2003.

[38] X. Liu and J. R. Banerjee, "An exact spectral-dynamic stiffness method for free flexural vibration analysis of orthotropic composite plate assemblies-part II: applications," *Composite Structures*, vol. 132, no. 15, pp. 1288–1302, 2015.